# Investigation of the low-energy kaons hadronic interactions in light nuclei by AMADEUS

K. Piscicchia*
On behalf of the AMADEUS collaboration
*kristian.piscicchia@lnf.infn.it

MIN16

31/7 – 2/8 2016, YITP, Kyoto University

# AMADEUS proposal

*Antikaon Matter At DAΦNE: Experiments with Unraveling Spectroscopy*

**AMADEUS collaboration**
**116 scientists from 14 Countries and 34 Institutes**

**lnf.infn.it/esperimenti/siddharta**
**and**
**LNF-07/24(IR) Report on lnf.infn.it web-page (Library)**

**AMADEUS started in 2005 and**
**was presented and discussed in all the LNF Scientific Committees**

**EU Fundings FP7 – I3HP2:**
**Network WP9 – LEANNIS;**
**WP24 (SiPM JRA);**
**WP28 (GEM JRA)**

# Why AMADEUS & DAΦNE?

# Why AMADEUS & DAΦNE?

## DAΦNE

Double ring $e^+ e^-$ collider working in C. M. energy of $\phi$, producing ≈ 600 $K^+ K^-$ /s

$\phi \rightarrow K^+ K^-$ (BR = (49.2 ± 0.6)%)

- low momentum Kaons ≈ 127 Mev/c
- back to back $K^+ K^-$ topology

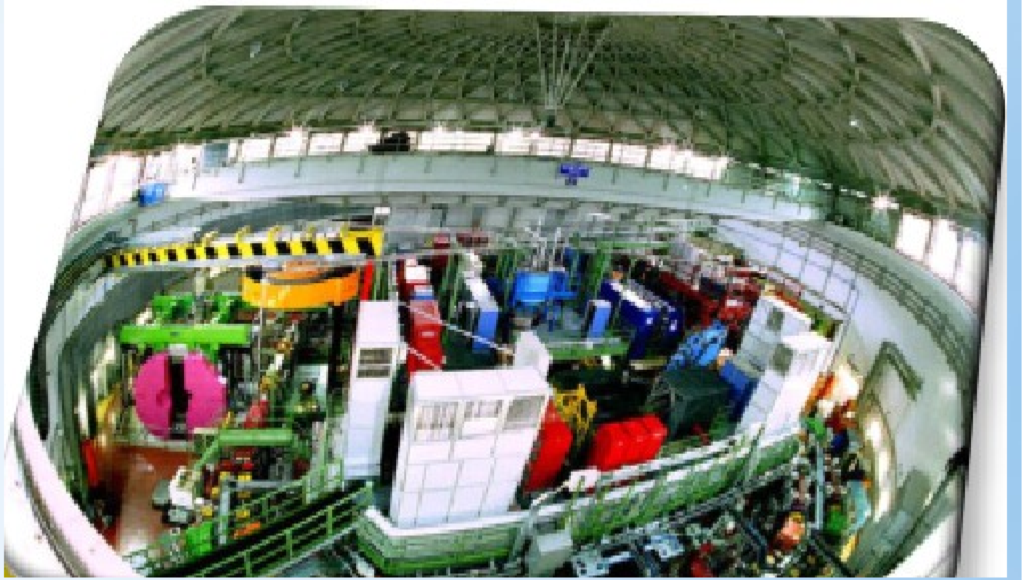

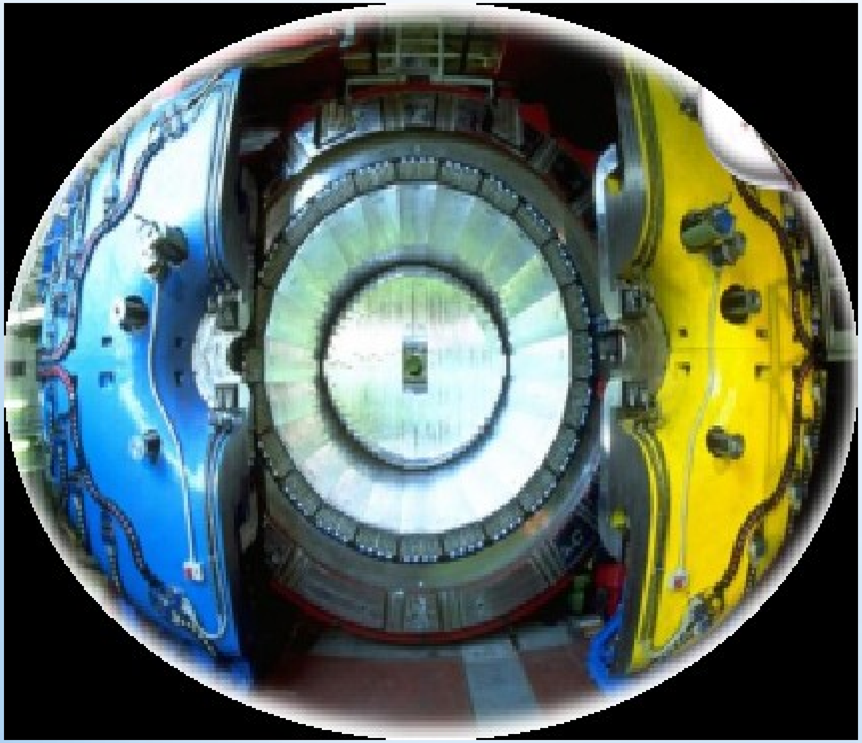

## KLOE

- 96% acceptance,
- optimized in the energy range of all charged particles involved
- good performance in detecting photons (and neutrons checked by kloNe group (M. Anelli et al., Nucl Inst. Meth. A 581, 368 (2007)))

# Why AMADEUS & DAΦNE?

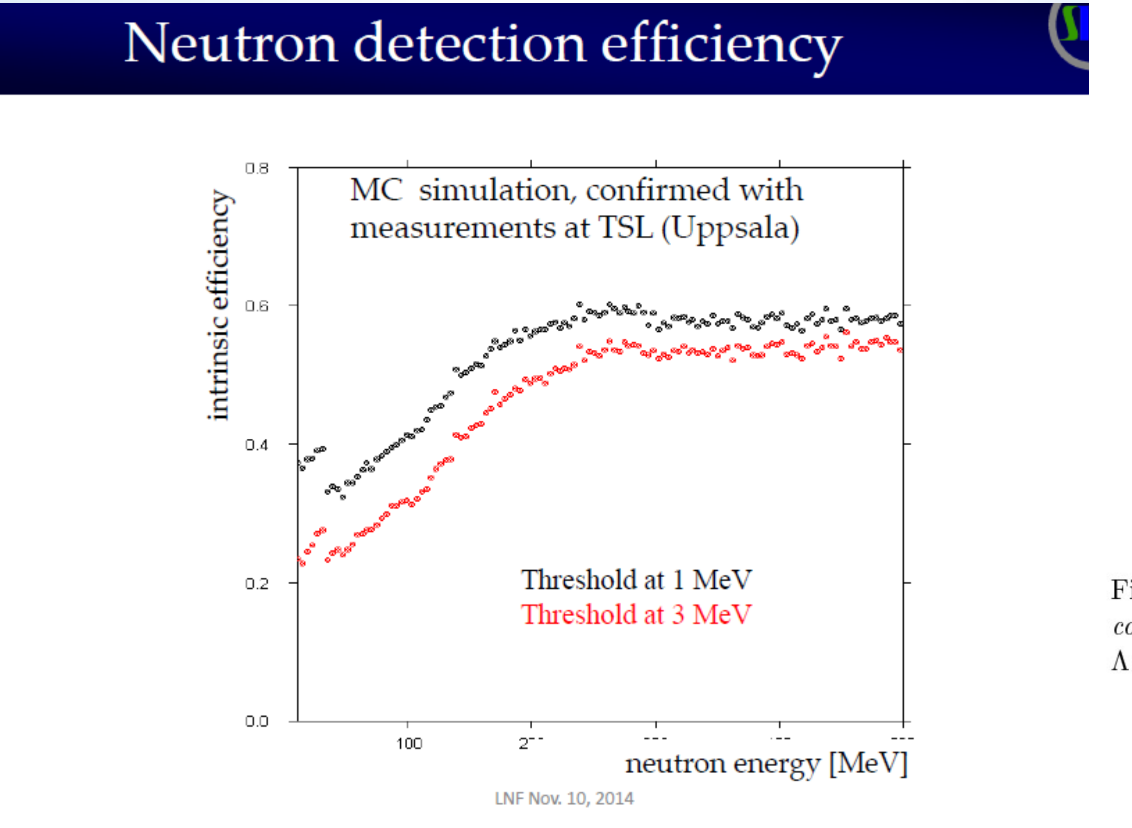


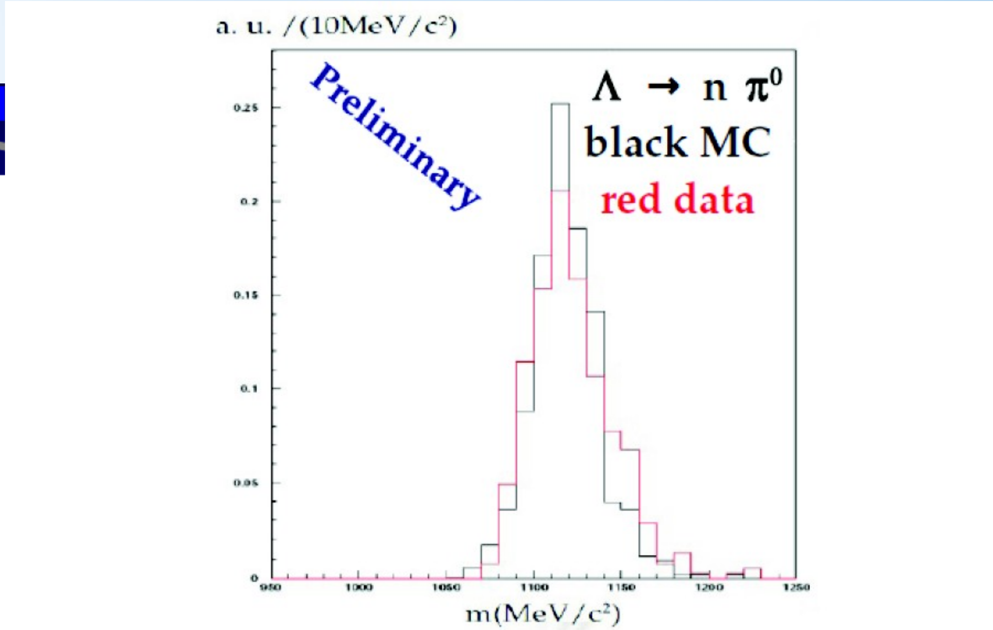


Fig. 1. $n\pi^0$ *invariant mass spectrum measured by the KLOE EMC, the red line corresponds to data, the black one corresponds to a Monte Carlo simulation of the* $\Lambda \to n\pi^0$ *decay, reconstructed in the KLOE calorimenter.*

## KLOE

- 96% acceptance,
- optimized in the energy range of all charged particles involved
- good performance in detecting photons (and neutrons checked by kloNe group (M. Anelli et al., Nucl Inst. Meth. A 581, 368 (2007)))

# AMADEUS target + tracking inside KLOE spectrometer

**Implementation of dedicated solid targets & cryogenic gaseous targets (H, d, $^{3}$He, $^{4}$He) inside the KLOE DC.**

**Nucl. Instrum. Meth. A671 (2012) 125-128**

**JINST 8 (2013) T05006**

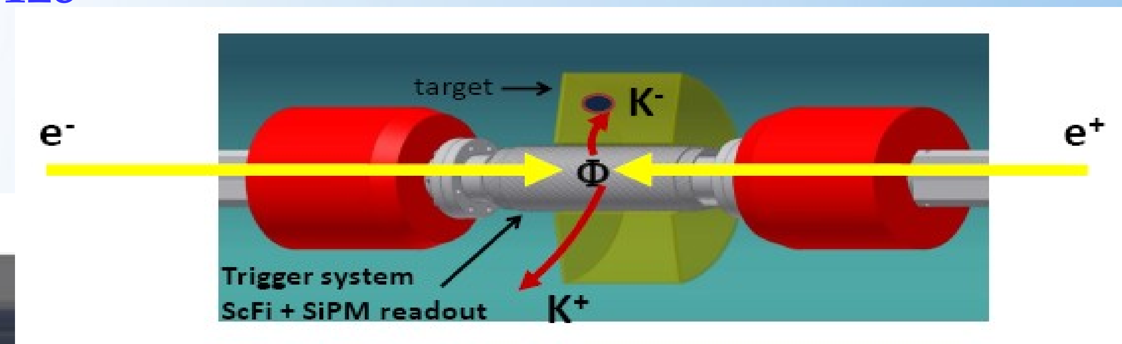


•The AMADEUS setup will be implemented in the 50 cm. gap in KLOE DC around the beam pipe:

- **Target** ( A gaseous He target for a first phase of study)
- **Trigger** (1 or 2 layers of ScFi surrounding the interaction point)

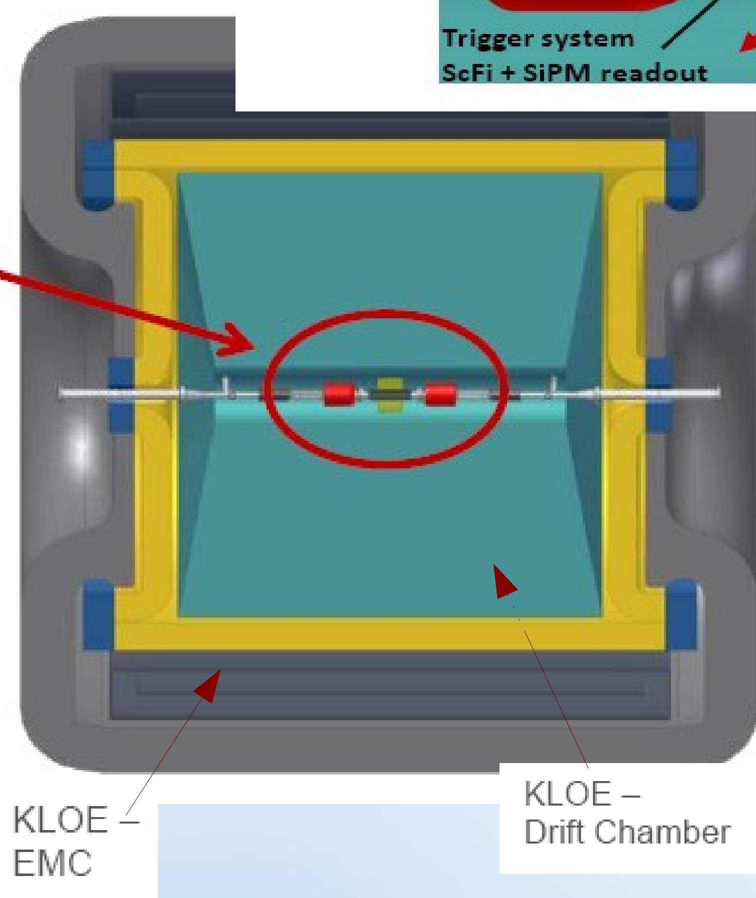


**R&D activity is ongoing**

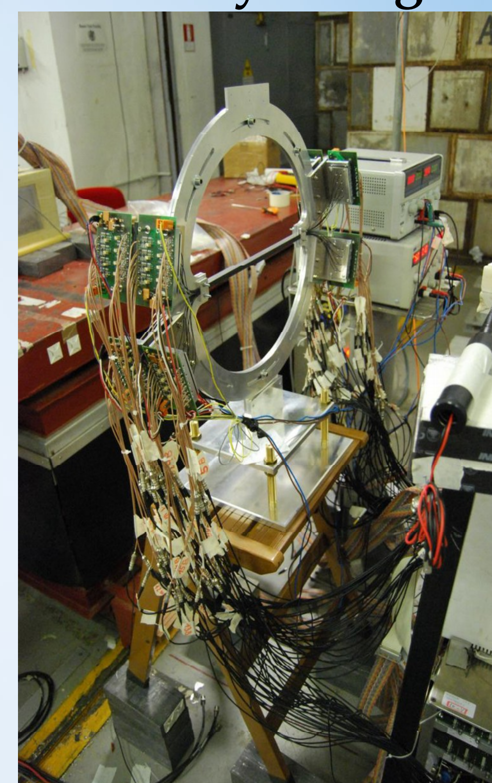

# KLOE electromagnetic calorimeter

**or re-using the calorimeter only, with a new tracking detector**

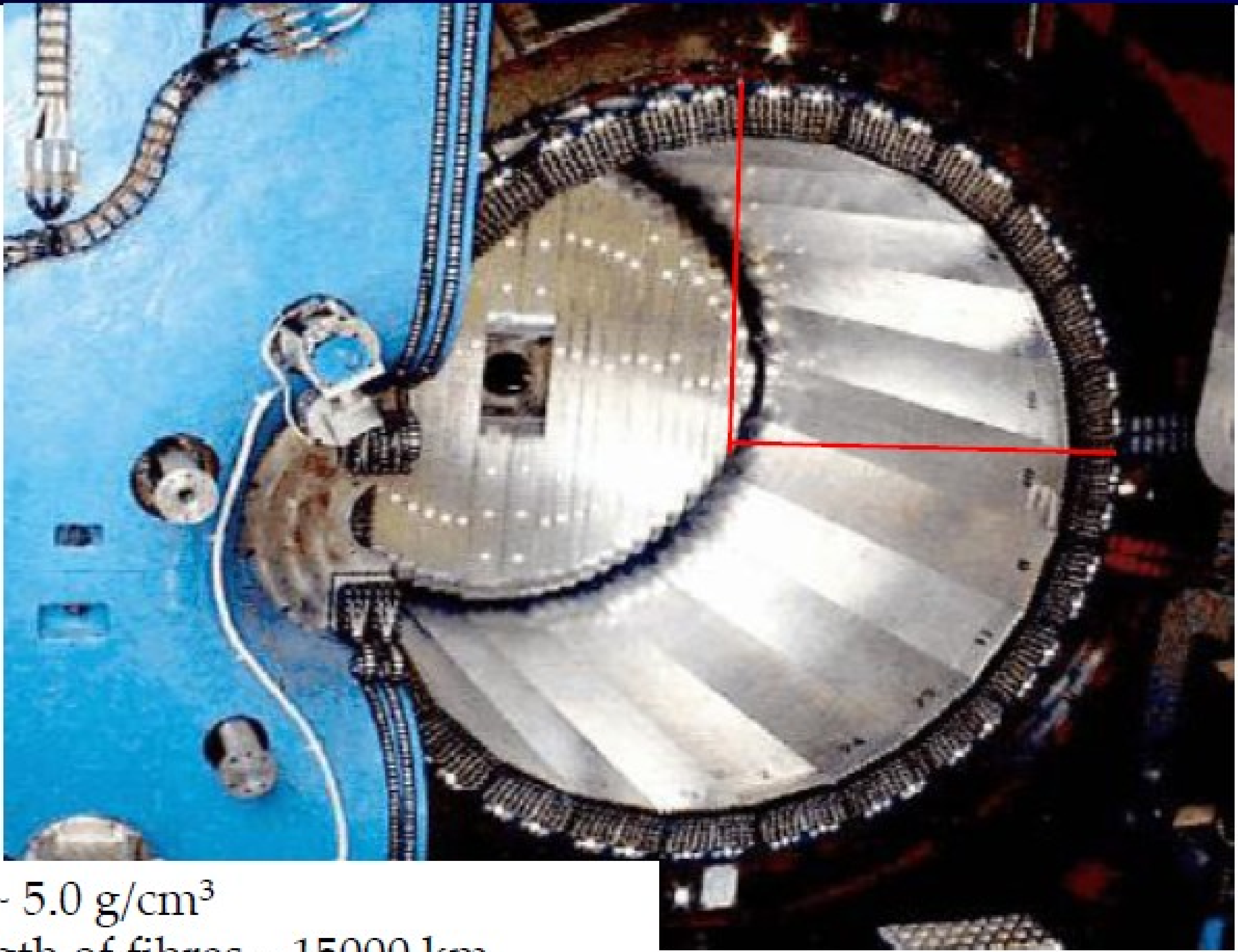

density ~ 5.0 g/cm$^3$
total length of fibres ~ 15000 km
read out by ~ 5000 mesh PM

# R&D – advanced setup

- **active target TPC with GEM technology, with 6000 pads**
  - ➢ R&D work within EU-FP7 HadronPhysics3

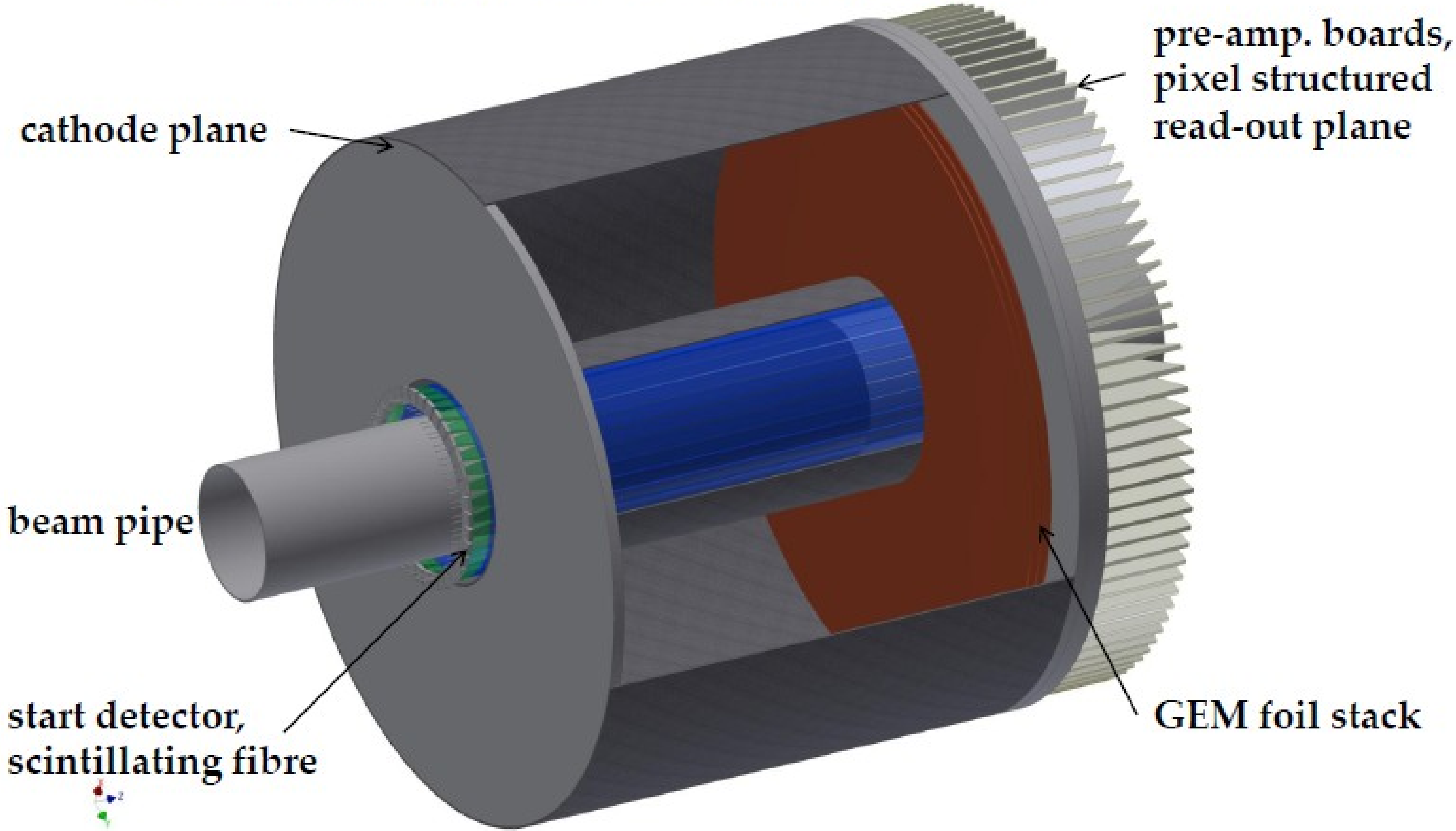

# “active” TPC-GEM test setup at LNF

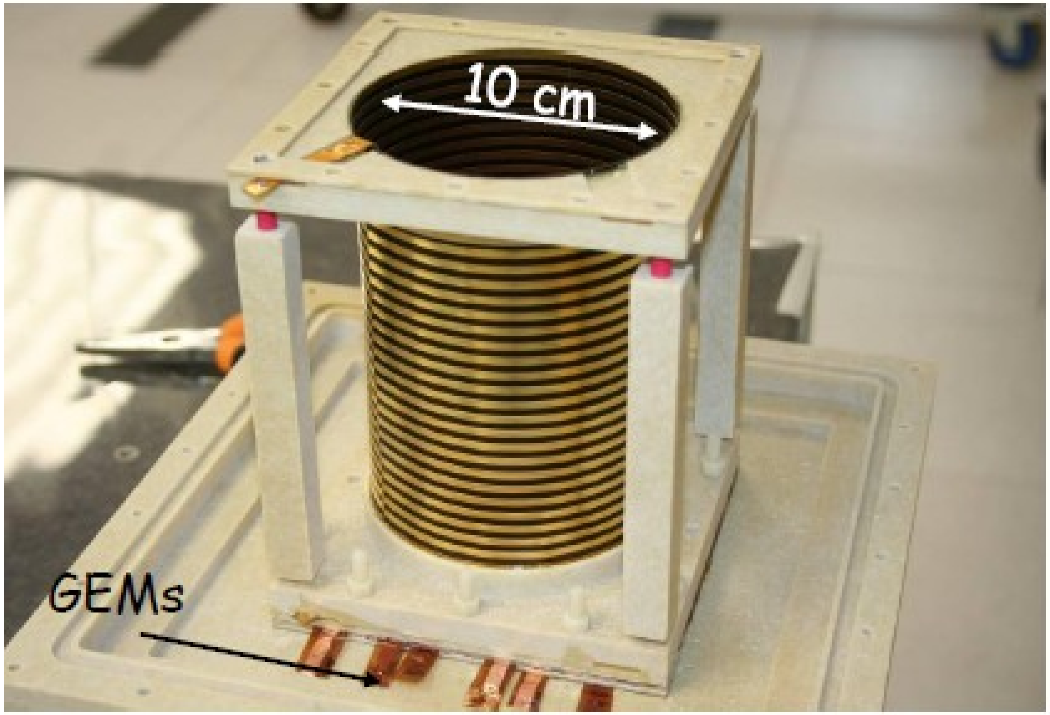


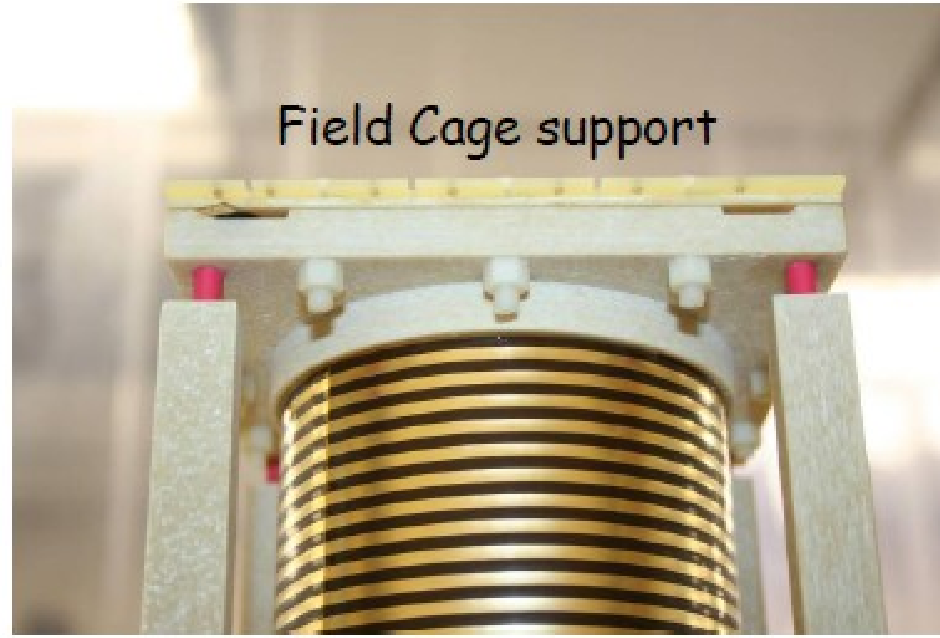


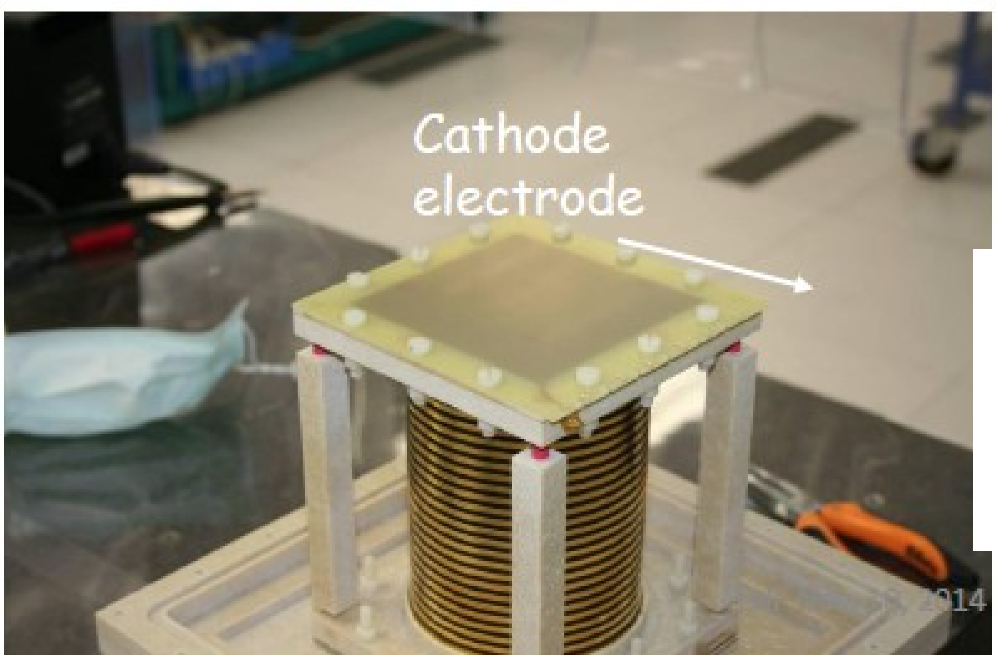


## Tests at PSI

Modern Instrumentation, 2015, 4, 32-41
Published Online July 2015 in SciRes. http://www.scirp.org/journal/mi
http://dx.doi.org/10.4236/mi.2015.43004

Scientific Research Publishing

**Performances of an Active Target GEM-Based TPC for the AMADEUS Experiment**

M.Poli Lener

# What to do meanwhile?

# $K^-$ absorption on light nuclei

## from the materials of the KLOE detector

DC gas (90% He, 10% $C_4H_{10}$) & DC wall (C + H)

AT-REST ($K^-$ absorbed from atomic orbit) or IN-FLIGHT ($p_K$~100MeV)

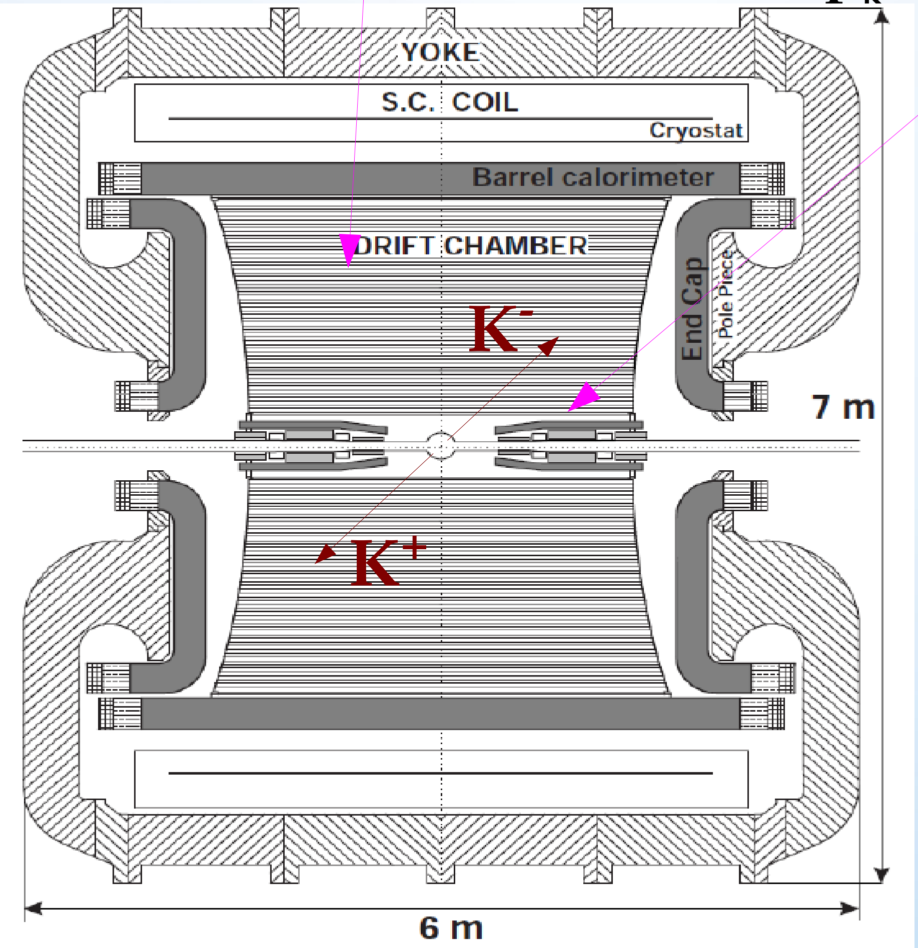


Advantage:
excellent resolution ..
$\sigma_{p\Lambda}$ = 0.49±0.01 MeV/c in DC gas
$\sigma_{m\gamma\gamma}$ = 18.3±0.6 MeV/$c^2$

Disadvantage:
Not dedicated target → different nuclei contamination → complex interpretation .. but → new features .. $K^-$ in flight absorption.

# The scientific goal of AMADEUS

Low energy QCD in strangeness sector is still waiting for experimental conclusive constrains on:

1) $\bar{K}$-N potential → how deep can an antikaon be bound in a nucleus?

- $U_{KN}$ strongly affects the position of the Λ(1405) state → we investigate it through $(\Sigma\text{-}\pi)^0$ decay --- Y π CORRELATION

- if $U_{KN}$ is strongly attractive then $K^-$ NN bound states should appear → we investigate through (Λ/Σ-N) decay --- Y N CORRELATION

2) Y-N potential → extremely poor experimental information from scattering data

- $U_{YN}$ determines the strength of the final state YN (elastic & inelastic) scattering in nuclear environment → could be tested by Y N CORRELATION

# $K^-$ - multi nucleon absorption and $K^-$ pp bound state search

# Σ0 p correlated production, goals of this analysis

## K- Absorption

- Pin down the contribution of the process:

$$K^- + NN \rightarrow \Sigma^0 + p$$

with respect to processes as:

$$K^- + NN \rightarrow \Sigma^0 + p \rightarrow p" + \Sigma^0" \; (FSI)$$

$$K^- + NNN \rightarrow \Sigma^0 + p + X$$

$$K^- + NNNN \rightarrow \Sigma^0 + p + X$$

## Kaonic Bound States

$$ppK^- \rightarrow \Sigma^0 + p$$

- Yield Extraction and Significance

# Final fit

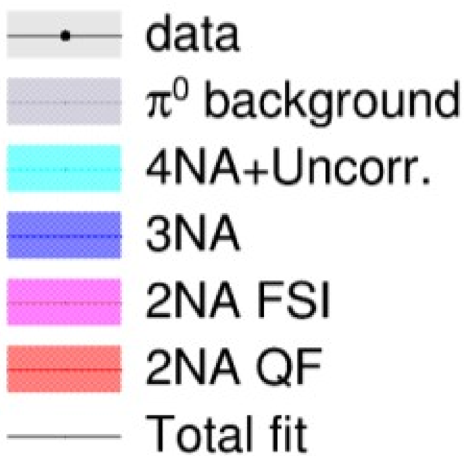


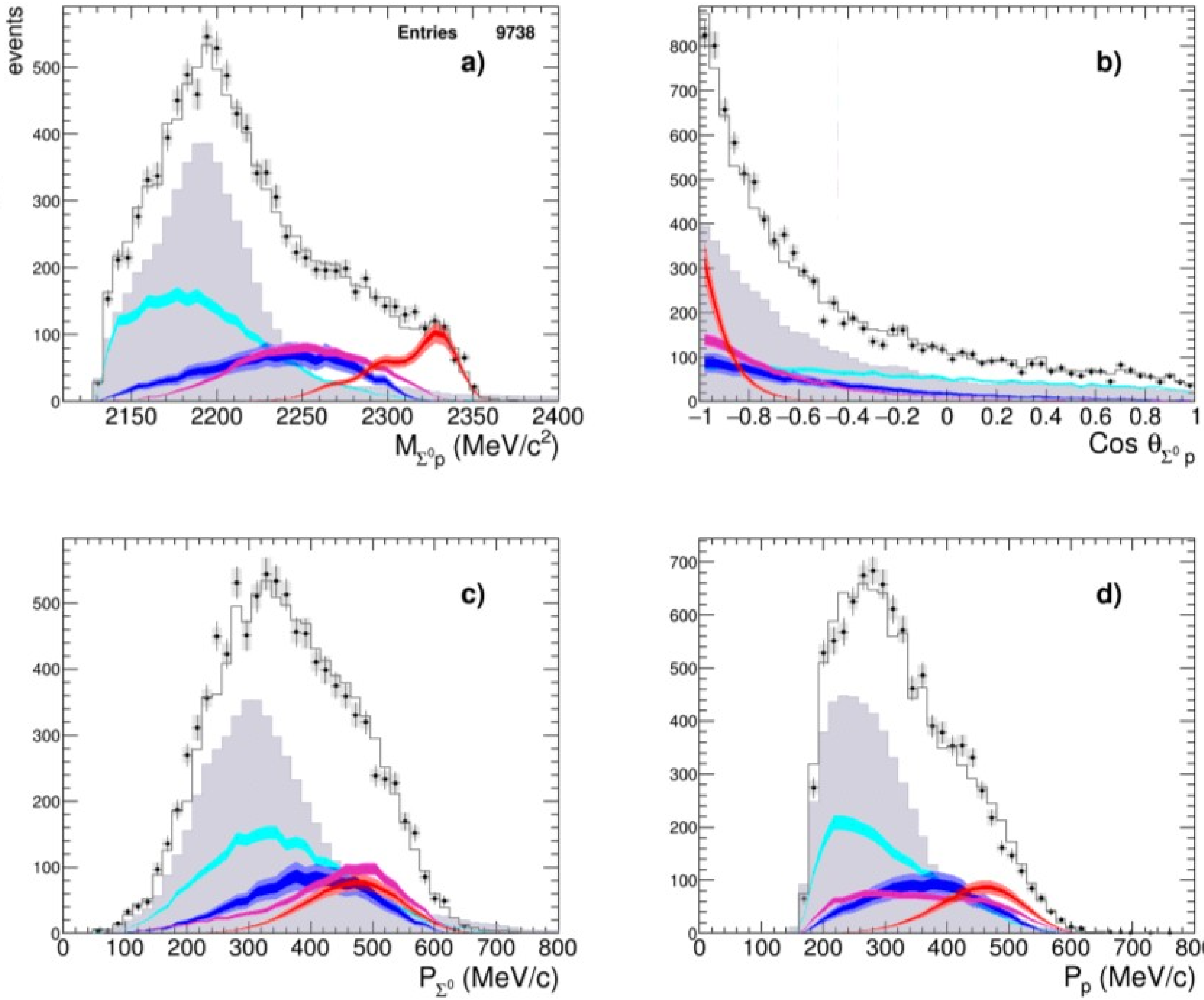


$$\chi^2 = 0.85$$

2NA-QF clearly separated From other processes

From the contributions to the fit, the yields are extracted for K- stop

# Absorption results

| | yield / $K^-_{stop} \cdot 10^{-2}$ | $\sigma_{stat} \cdot 10^{-2}$ | $\sigma_{syst} \cdot 10^{-2}$ |
|---|---|---|---|
| 2NA-QF | 0.127 | $\pm$ 0.019 | $^{+0.004}_{-0.008}$ |
| 2NA-FSI | 0.272 | $\pm$ 0.028 | $^{+0.022}_{-0.023}$ |
| Tot 2NA | 0.376 | $\pm$ 0.033 | $^{+0.023}_{-0.032}$ |
| 3NA | 0.274 | $\pm$ 0.069 | $^{+0.044}_{-0.021}$ |
| Tot 3body | 0.546 | $\pm$ 0.074 | $^{+0.048}_{-0.033}$ |
| 4NA + bkg. | 0.773 | $\pm$ 0.053 | $^{+0.025}_{-0.076}$ |

...is there room for the signal of a **ppK- bound state**?

# Fit with ppK-

Best solution:
(best $\chi 2$ and higher yield)

**- B.E. = 45 MeV/c2**
**- Width = 30 MeV/c2**

$$\chi^2 = 0.807$$

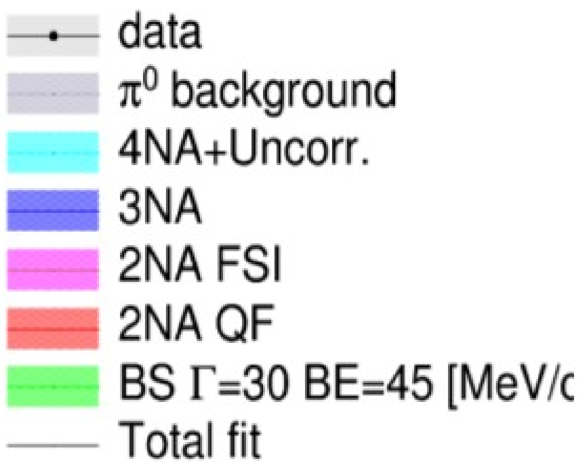


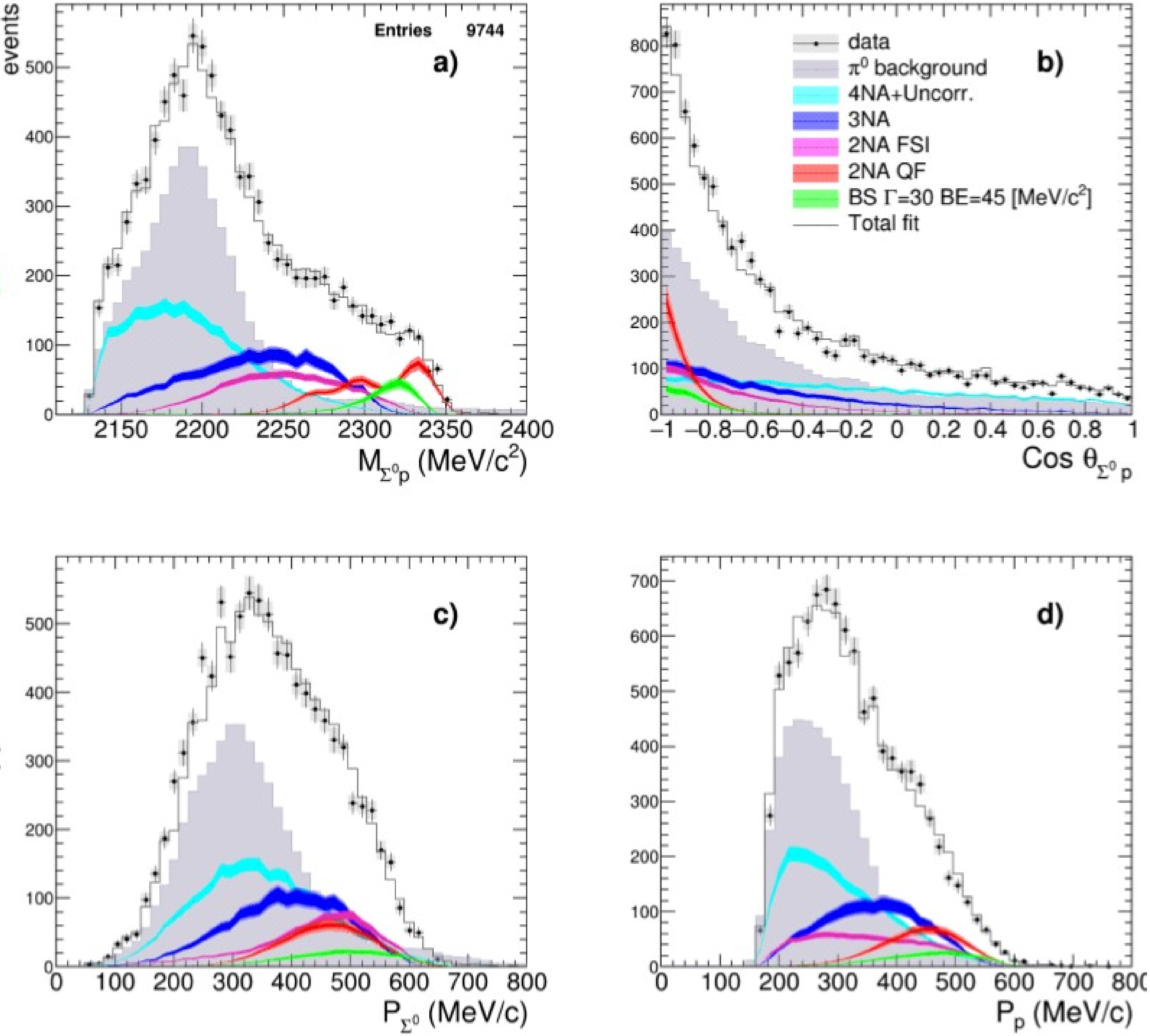

# Evaluation of the significance of the ppK- signal

For B.E. = 45 MeV/c2, Width = 30 MeV/c2

$$Yield/K^-_{stop} = (0.044 \pm 0.009 stat^{+0.004}_{-0.005} syst) \cdot 10^{-2}$$

F-test to evaluate the addition of an extra parameter to the fit:

Significance of “signal” hypothesis w.r.t “Null-Hypothesis” (no bound state)

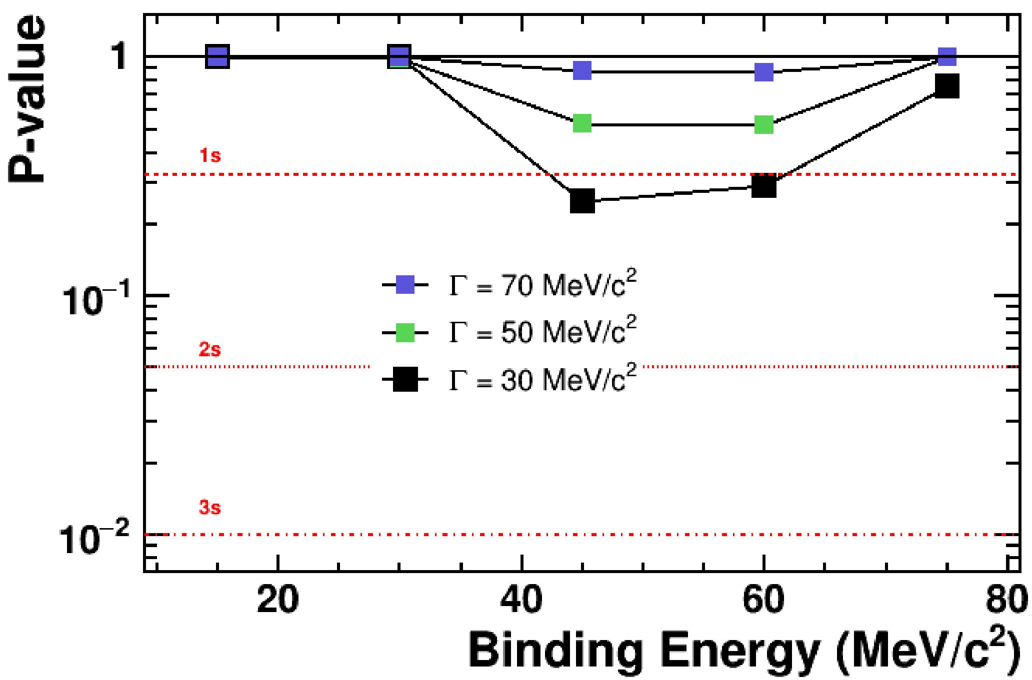

# Conclusions

- 2NA-QF yield

| | yield / $K^{-}_{stop} \cdot 10^{-2}$ | $\sigma_{stat} \cdot 10^{-2}$ | $\sigma_{syst} \cdot 10^{-2}$ |
|---|---|---|---|
| 2NA-QF | 0.127 | $\pm$ 0.019 | $^{+0.004}_{-0.008}$ |

- Bound state ppK- yield for B.E. 45 MeV/c2 and Width 30 MeV/c2

$$Yield/K^{-}_{stop} = (0.044 \pm 0.009 stat^{+0.004}_{-0.005} syst) \cdot 10^{-2}$$

- the significance of the ppK- signal is of 1σ according to F-test

O. Vazquez Doce et al., Physics Letters B 758 (2016) 134

$K^- \, {}^4He \rightarrow \Lambda t$

**4NA  cross section and yield**

# Λt available data

Available data:

- in Helium :

  - bubble chamber experiment
  [M.Roosen, J.H. Wickens, Il Nuovo Cimento 66, (1981), 101]
  $K^-$ stopped in liquid helium, Λ dn/t search. 3 events compatible with the Λt kinematics were found

  **BR**($K^{-4}He \rightarrow \Lambda t$) **= (3 ± 2) × $10^{-4}$ /$K_{stop}$** global, no 4NA

- Solid targets

  - FINUDA [Phys.Lett. B669 (2008) 229]
  (40 events in different solid targets)

- T.Suzuki et al. Three- and four-nucleon absorption processes observed in the K −4He reaction at rest , arXiv:1009.5082v1 [nucl-ex] 26 Sep 2010 .

# Λt available data

FINUDA presented [Phys.Lett.B (2008) 229]:

- a study of Λ vs t momentum correlation and an opening angle distribution
- **40 events** collected and added together coming from different targets ($^{6,7}$Li, $^{9}$Be)

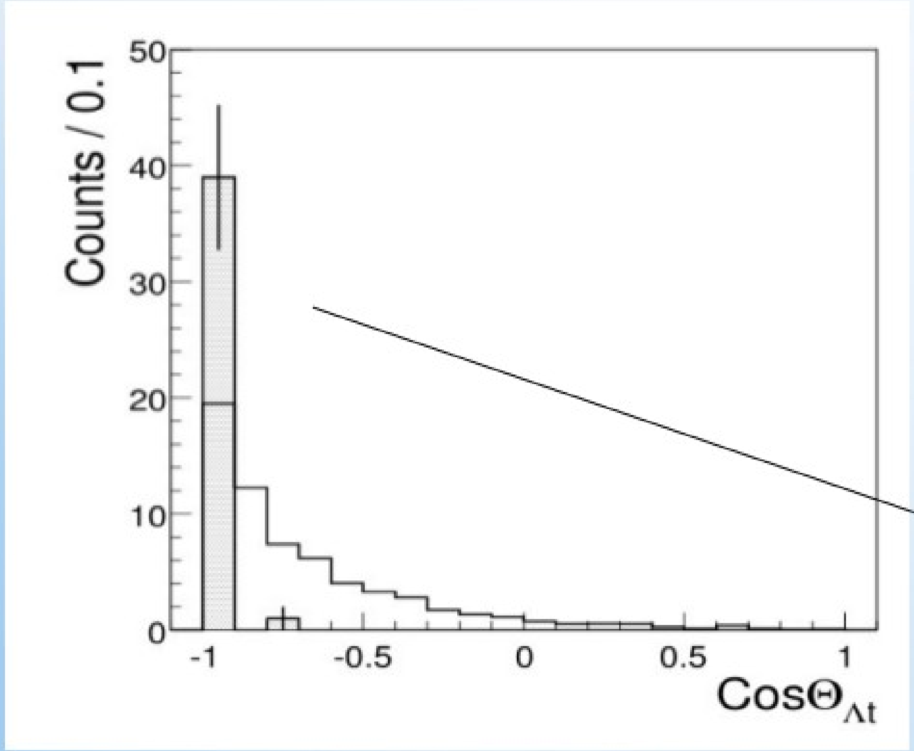


**Filled histogram= data**

**Open histogram = Phase space simulation**

**( K- A → Λ t N A' )**

Unclear back to back topology

Λt emission yield → $10^{-3} – 10^{-4} / K^{-}_{stop}$

global, no 4NA

**Experimental data only back-to-back**

# Λt correlation studies in $^4He$ from the DC gas : contributing processes

**single nucleon absorption (1NA)**

$$K^- \, {}^4He \rightarrow \Lambda \, \pi^0 \, t_{res}$$

$$K^- \, {}^4He \rightarrow \Sigma^0 \pi^0 \, t_{res} \quad , \quad \Sigma^0 \rightarrow \Lambda\gamma$$

**conversion on triton:**

$$K^- \, {}^4He \rightarrow \Sigma^0 \pi^0 \, t \quad , \quad \Sigma^0 t \, / \, \Lambda t$$

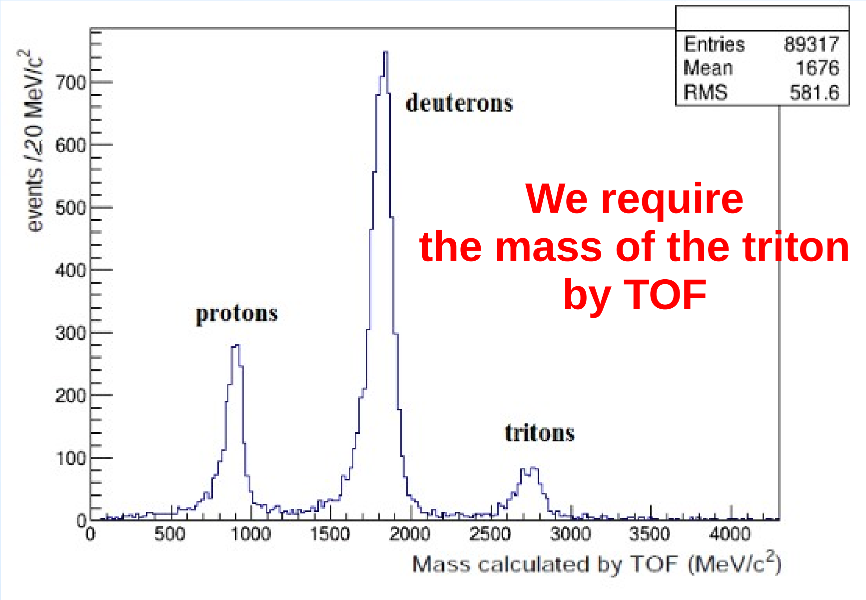


**Tritons are spectators, too low momentum: $p_t$ ~ Fermi momentum**

**<u>lower then the calorimeter threshold</u> ($p_t$ ~ 500 MeV/c)**

**<u>checked by MC simulations</u>**

**4NA processes – $K^-$** absorbed by the **α particle:**

$$K^- \, {}^4He \rightarrow \Lambda t$$

$$K^- \, {}^4He \rightarrow \Sigma^0 t \quad , \quad \Sigma^0 \rightarrow \Lambda\gamma$$

**conversion is suppressed**
**By the**
**$\Sigma^0$- t**
**Back to back topology!**

# MC simulations:  efficiency & resolution

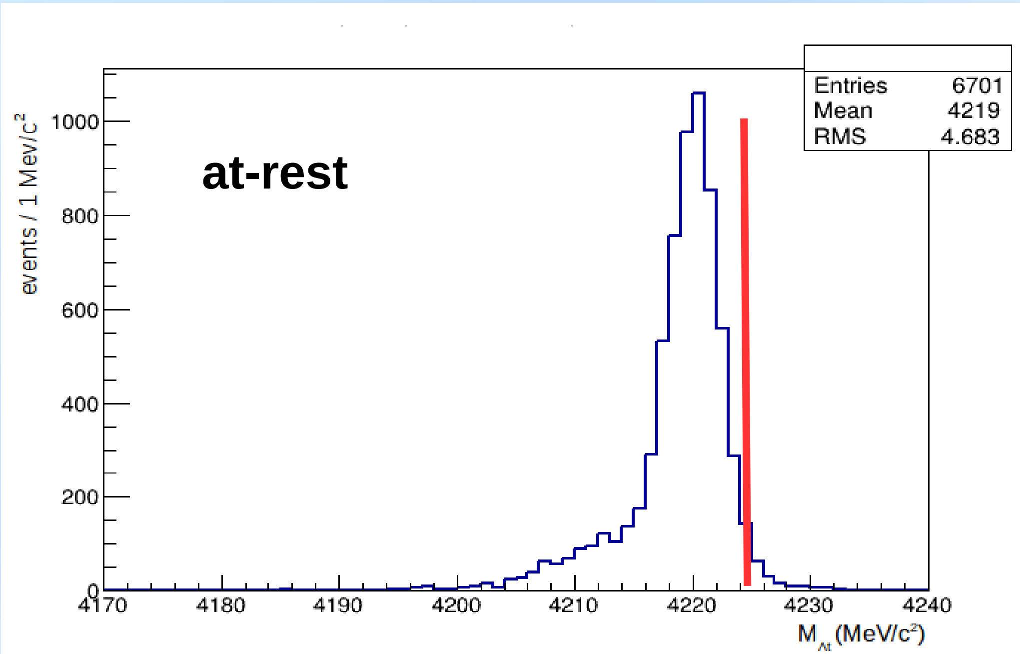


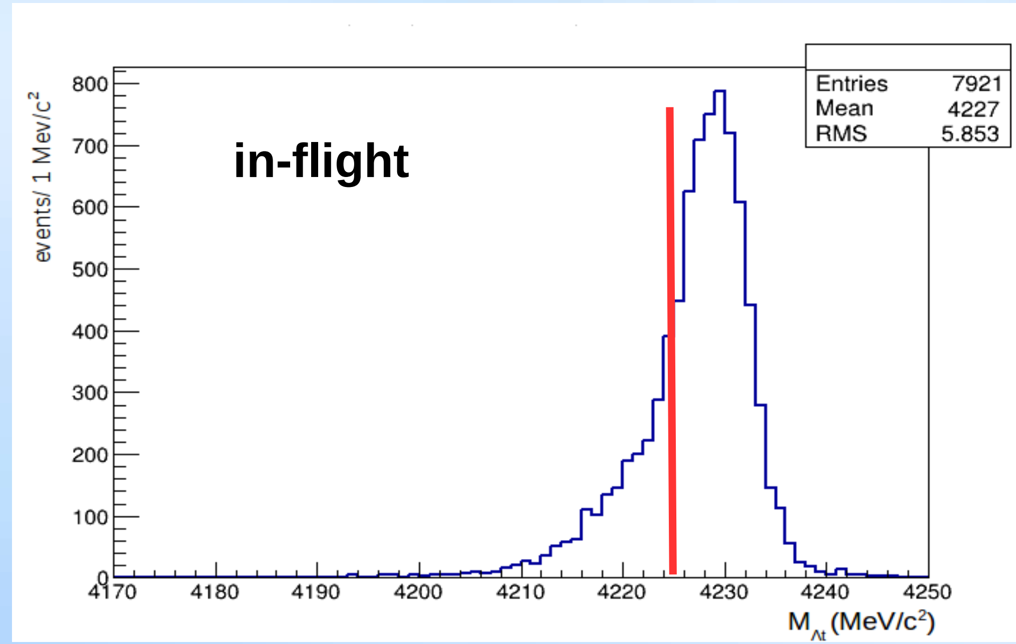


**mass threshold at-rest**

**$M_{\Lambda t}$ invariant mass resolution  =  2.2 MeV/c$^2$**

**averall <u>detection + reconstruction efficiency</u> for 4NA direct Λt production :**

$$\epsilon_{4\mathrm{NA},ar,\Lambda t} = 0.0493 \pm 0.0006 \quad ; \quad \epsilon_{4\mathrm{NA},if,\Lambda t} = 0.0578 \pm 0.0006,$$

**at-rest** **in-flight**

Preliminary

# Λt correlation studies in $^4$He: mass, momentum and angle simulataneous fit

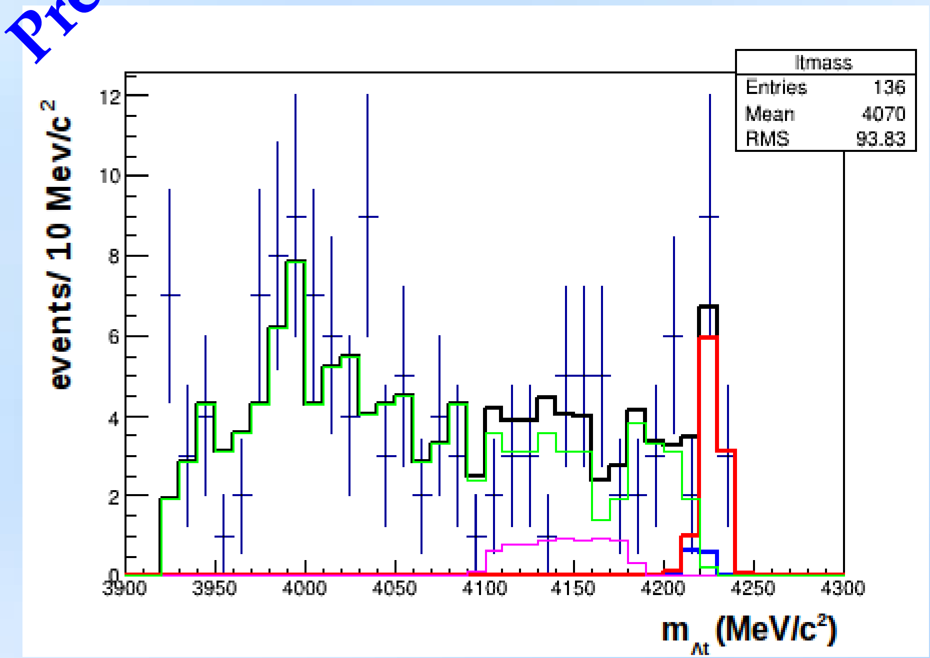


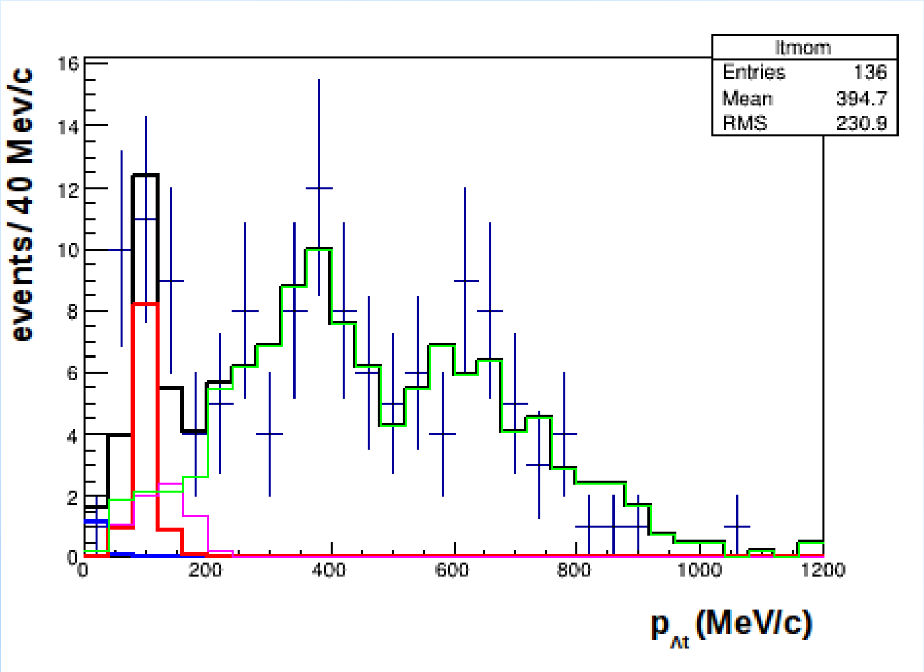


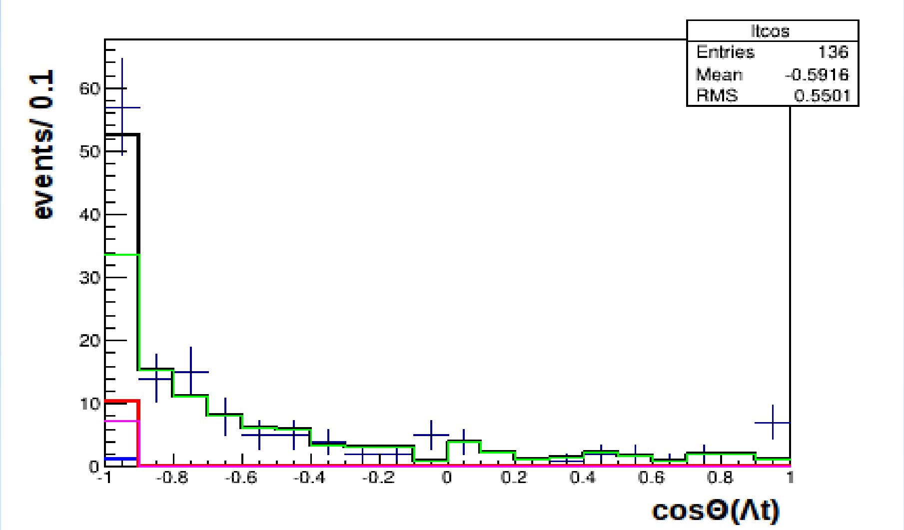


data

--- carbon data from DC wall

--- 4NA $K^- \, ^4He \rightarrow \Lambda t$ in flight MC

--- 4NA $K^- \, ^4He \rightarrow \Lambda t$ at rest MC

--- 4NA $K^- \, ^4He \rightarrow \Sigma^0 t$ , $\Sigma^0 \rightarrow \Lambda\gamma$ MC

--- 4NA $K^- \, ^4He \rightarrow \Sigma^0 t$ , $\Sigma^0 \rightarrow \Lambda\gamma$ MC

Preliminary

# Λt correlation studies in $^4$He: preliminary mass and angle momentum simulataneous fit

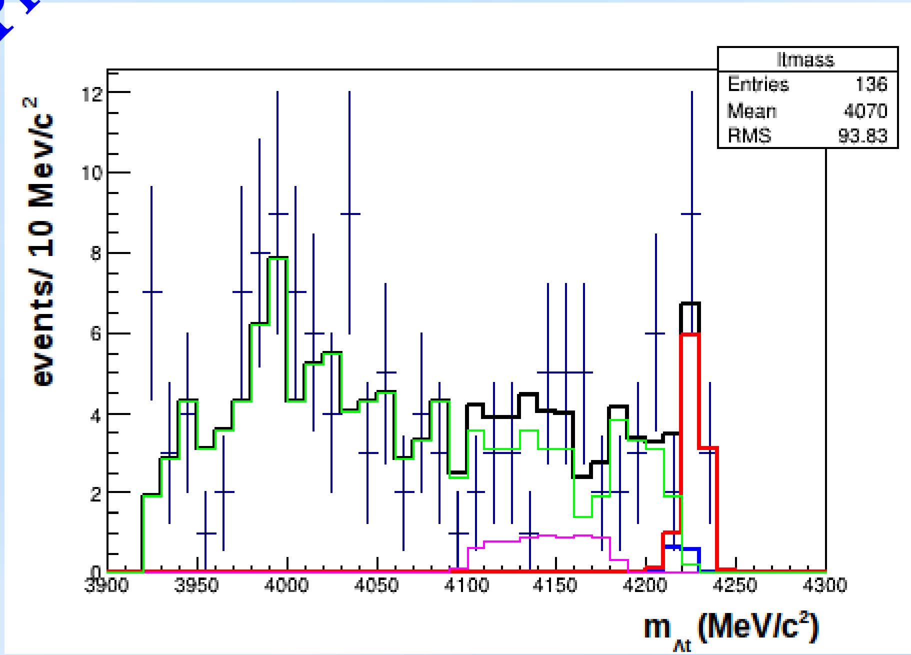


| Contribution to the spectra | Parameter value |
|---|---|
| $K^{-4}$He $\rightarrow \Lambda t$ at rest | $0.01 \pm 0.01$ |
| $K^{-4}$He $\rightarrow \Lambda t$ in-flight | $0.09 \pm 0.02$ |
| $K^{-4}$He $\rightarrow \Sigma^0 t$ in-flight | $0.05 \pm 0.03$ |
| $K^{-12}$C $\rightarrow \Lambda t$ experimental distribution from the carbon DC wall | $0.85 \pm 0.06$ |
| $\chi^2$ / ndf | 0.654 |

parameters giving the contribution of the each process

data

--- carbon data from DC wall

--- 4NA K$^-$ $^4$He → Λt in flight MC

--- 4NA K$^-$ $^4$He → Λt at rest MC

--- 4NA K$^-$ $^4$He → Σ$^0$t , Σ$^0$ → Λγ MC

--- 4NA K$^-$ $^4$He → Σ$^0$t , Σ$^0$ → Λγ MC

Total number of events = 136

4NA K$^-$ $^4$He → Λt at rest → 1 ± 1 events

4NA K$^-$ $^4$He → Λt in flight → 12 ± 3 events

**BR**(K$^-$$^4$He(4NA) → Λt) **< 1.3 × 10$^{-4}$ /K$_{stop}$**

σ(100 ± **19** MeV/c) (K$^-$$^4$He(4NA) → Λt) **=**

**= (0.42 ± 0.13(stat) $^{+0.01}_{-0.02}$ (syst)) mb**

# $K^-$ - N single nucleon absorption processes

# Λ(1405) case

- Chiral unitary models: Λ(1405) is an I = 0 quasibound state emerging from the coupling between the $\bar{K}N$ and the Σπ channels. Two poles in the neighborhood of the Λ(1405):

*two poles*: about 1420 ; about = 1380 )MeV    Phys. Lett. B 500 (2001), Phys. Rev. C 66 (2002), (Nucl. Phys. A 725(2003) 181) .. many others .. (Nucl. Phys. A881, 98 (2012)) .. others

mainly coupled to $\bar{K}N$ (about 1420)    mainly coupled to Σπ (about 1380) → line-shape depends on production mechanism

- Akaishi-Esmaili-Yamazaki phenomenological potential

Phys. Lett. B 686 (2010) 23-28 Confirmation of single pole ansatz? ⟶

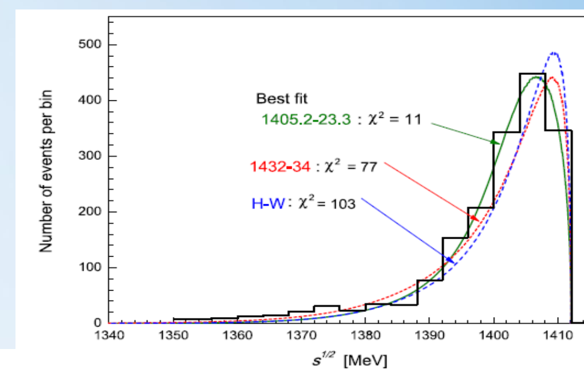


Fig. 6. Detailed differences in $M_{\Sigma\pi}$ spectra among the Hyodo–Weise prediction and the present model predictions.

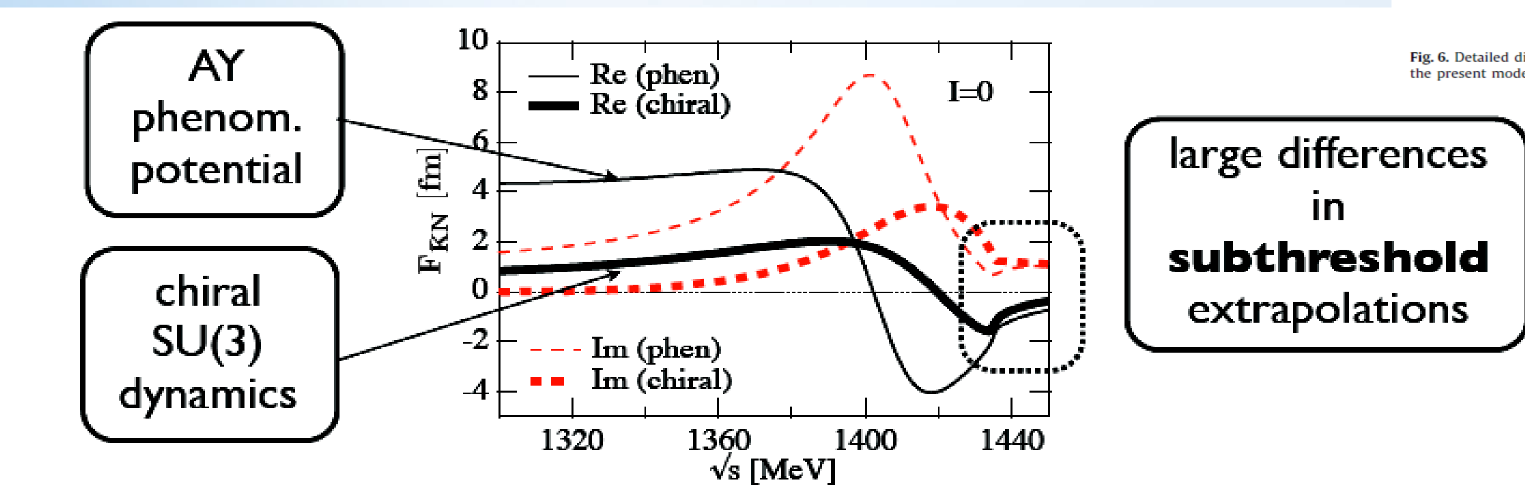


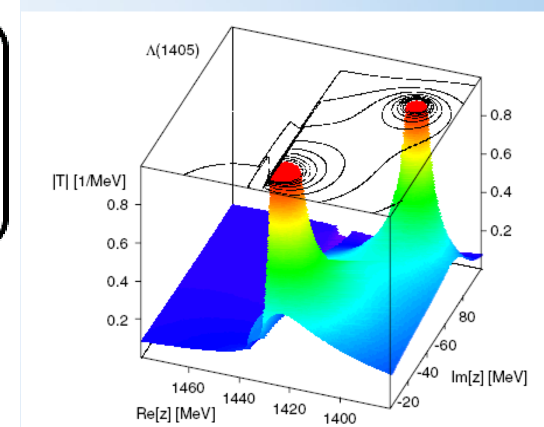


- **Chiral dynamics** predicts significantly **weaker attraction** than AY (local, energy independent) potential in **far-subthreshold** region

# Λ(1405) case

- Chiral unitary models: Λ(1405) is an I = 0 quasibound state emerging from the coupling between the $\bar{K}N$ and the Σπ channels. Two poles in the neighborhood of the Λ(1405):

*two poles*: about 1420 ; about = 1380 )MeV

Phys. Lett. B 500 (2001), Phys. Rev. C 66 (2002), (Nucl. Phys. A 725(2003) 181) .. many others .. (Nucl. Phys. A881, 98 (2012)) .. others

mainly coupled to $\bar{K}N$ mainly coupled to Σπ → line-shape depends on production mechanism

- Akaishi-Esmaili-Yamazaki phenomenological potential

Phys. Lett. B 686 (2010) 23-28 Confirmation of single pole ansatz?

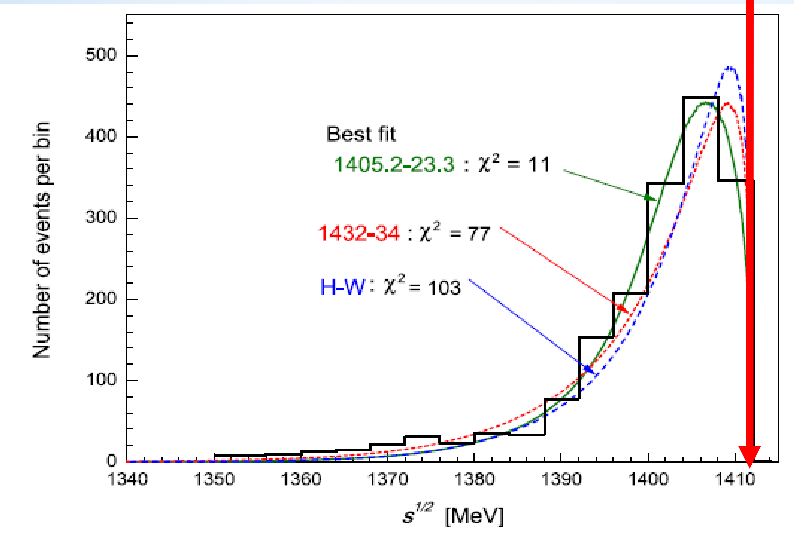


Fig. 6. Detailed differences in $M_{\Sigma\pi}$ spectra among the Hyodo–Weise prediction and the present model predictions.

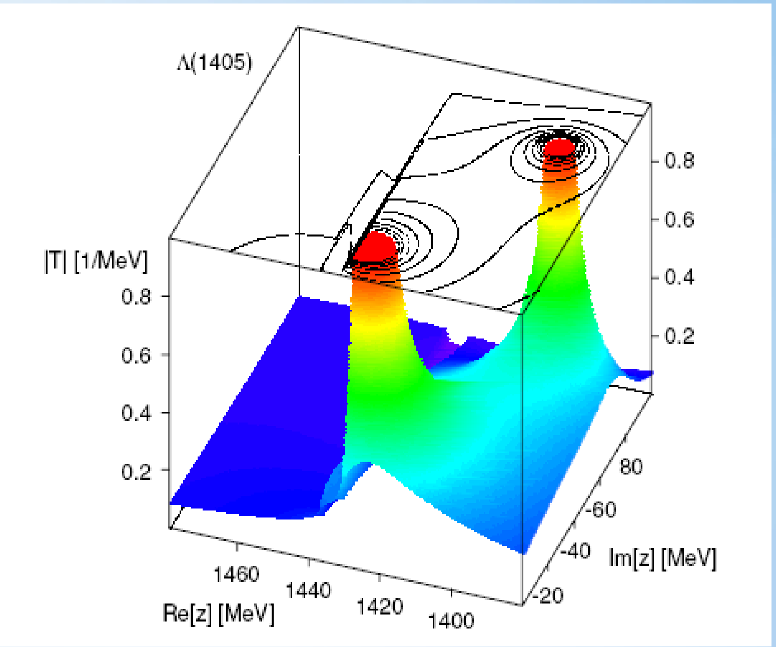


CUT AT THE ENERGY LIMIT AT-REST ?

NON RESONANT SHAPE ?

# $\Lambda(1405)$ case

Phys.Rev.Lett.95:052301,2005

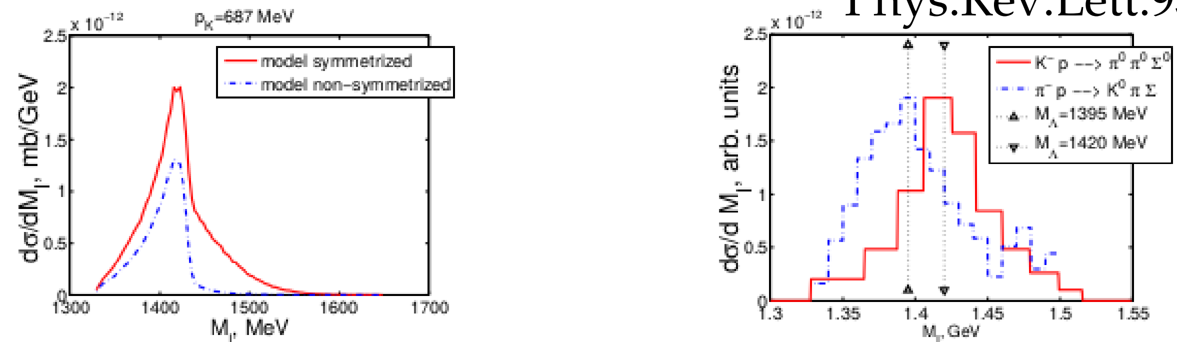


FIG. 4: Theoretical ($\pi^0\Sigma^0$) invariant mass distribution for an initial kaon lab momenta of 687 MeV. The non-symmetrized distribution also contains the factor 1/2 in the cross section.

FIG. 5: Two experimental shapes of $\Lambda(1405)$ resonance. See text for more details.

$\mathbf{p_{\pi 0}}$ **resolution**: $\sigma_p \approx 12$ MeV/c

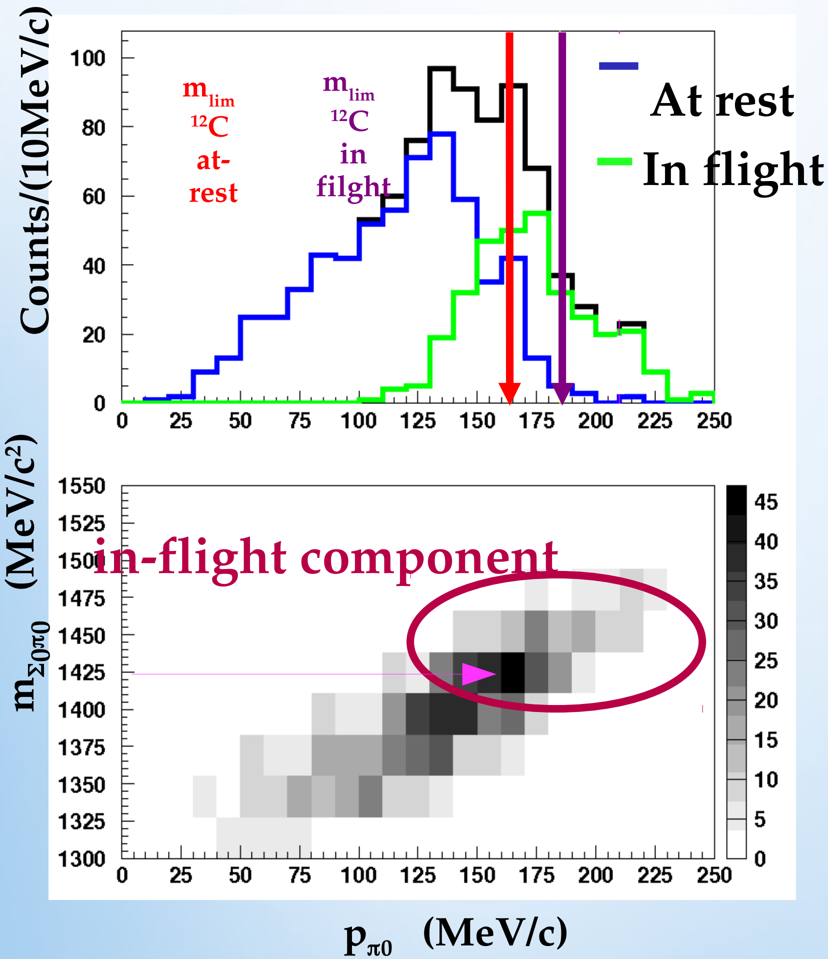


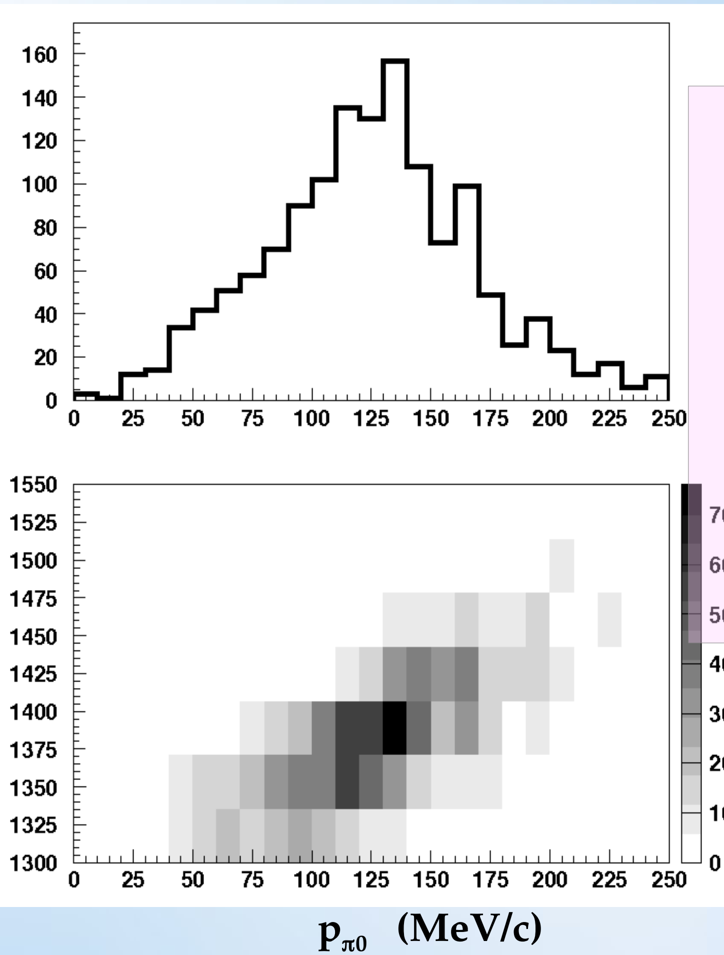


IN-FLIGHT

K- 12C

opens a window

between 1416 MeV

and K-Nth

# Complex interpretation due to K- H absorptions ongoing with the collaboration of A. Cieply (UJF, Prague)

$p_{\pi 0}$ **resolution**: $\sigma_p \approx 12$ MeV/c

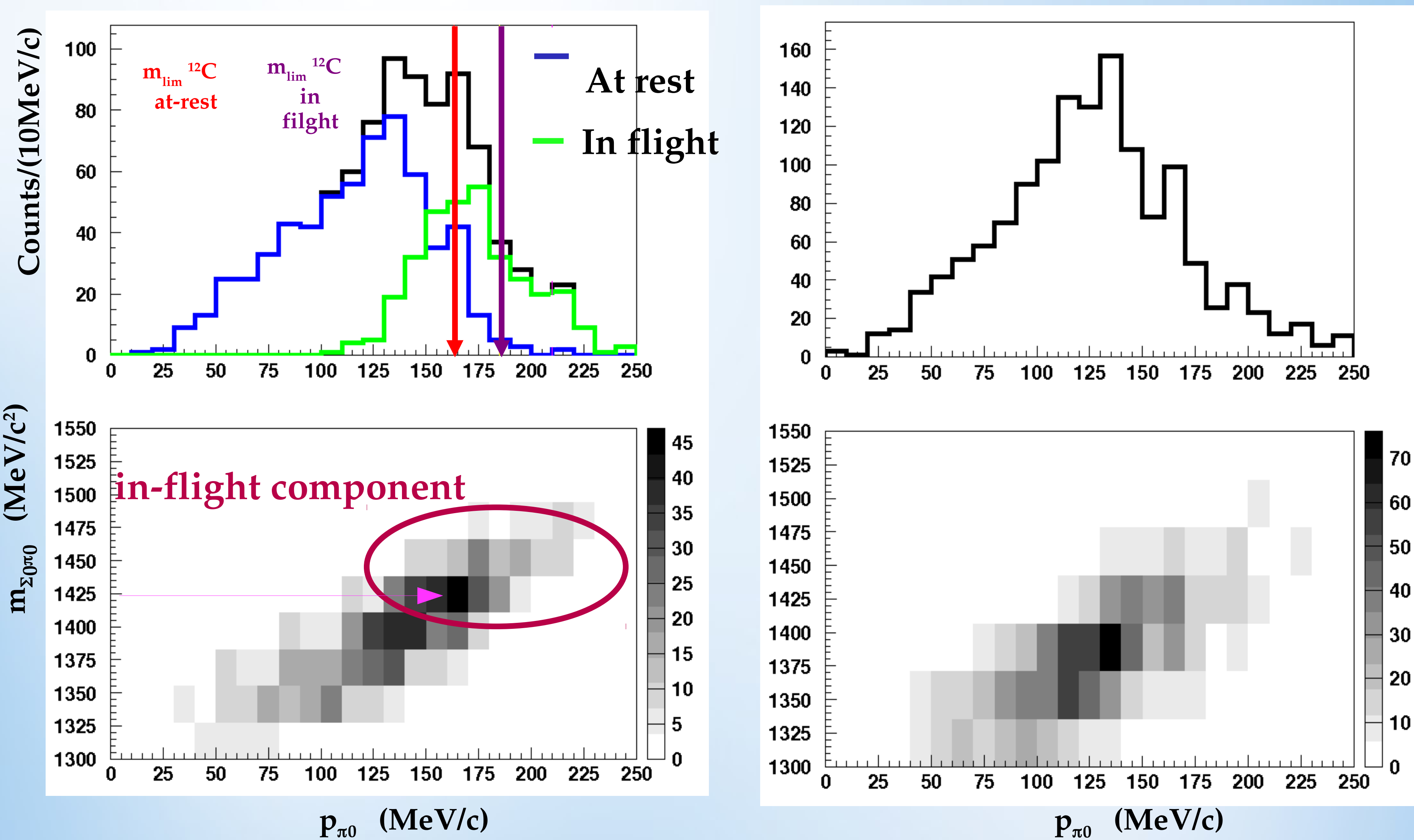

# $\Sigma^+\pi^-$ correlation

$K^- p \rightarrow \Sigma^+ \pi^-$ detected via: $(p\pi^0)\ \pi^-$

**Possibility to disentangle: Hydrogen, in-flight, at-rest, $K^-$ capture**

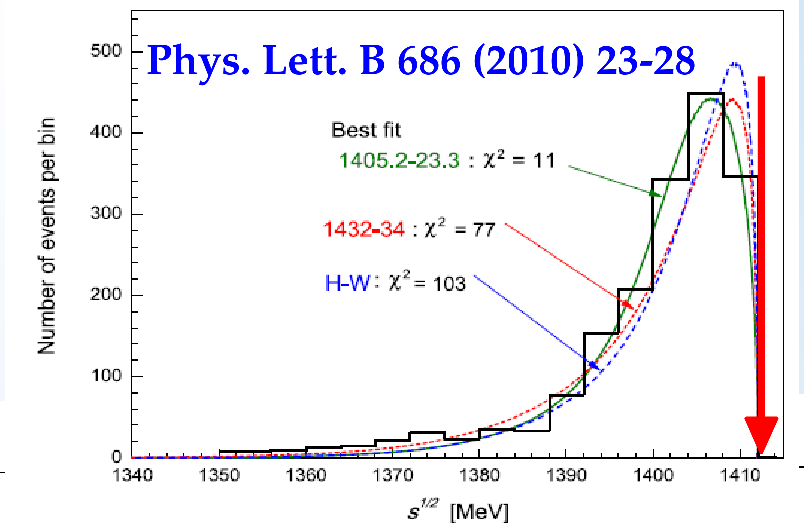


Fig. 6. Detailed differences in $M_{\Sigma\pi}$ spectra among the Hyodo–Weise prediction and the present model predictions.

$p_{\pi^-}$ resolution: $\sigma_p \approx 1$ MeV/c

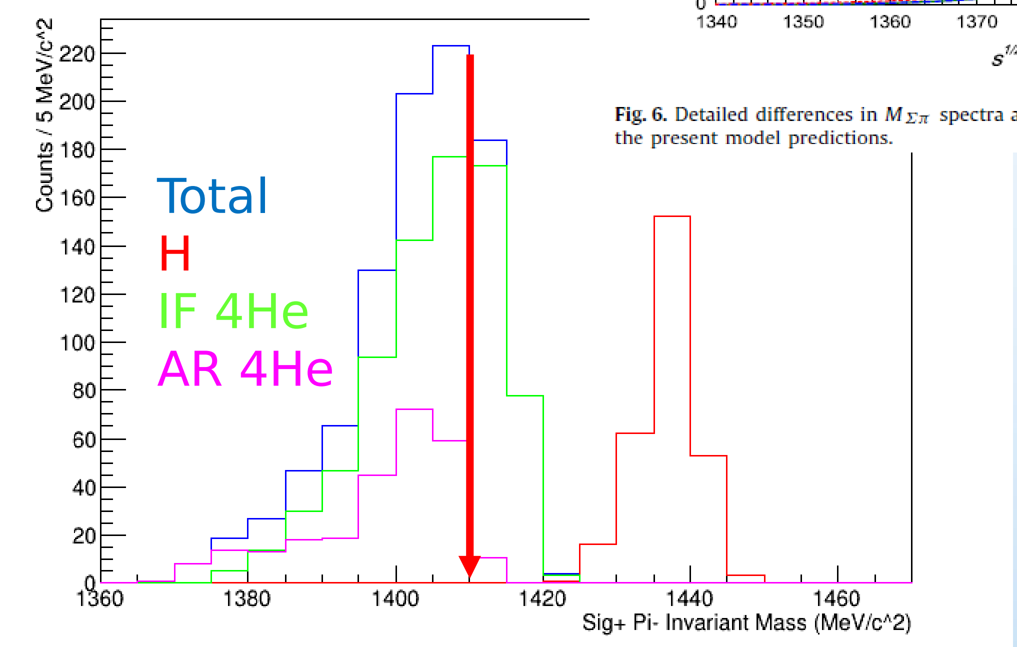


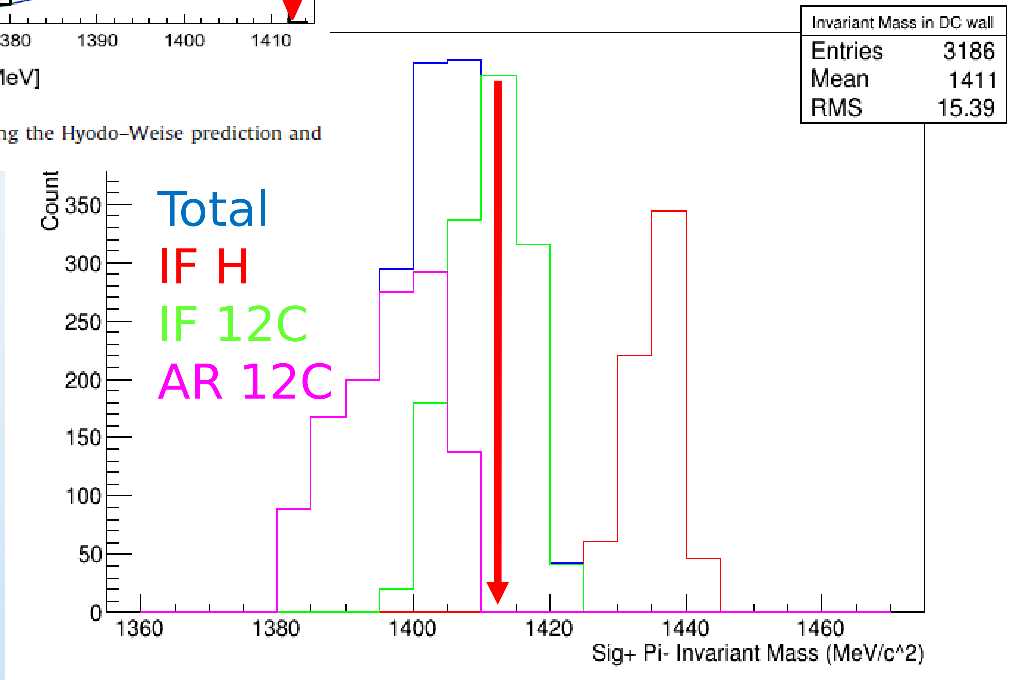

# $\Sigma^+\pi^-$ correlation

$K^- p \rightarrow \Sigma^+ \pi^-$ detected via: $(p\pi^0)\ \pi^-$

**Possibility to disentangle: Hydrogen, in-flight, at-rest, $K^-$ capture**

**if resonant production contribution is important a high mass component appears!**

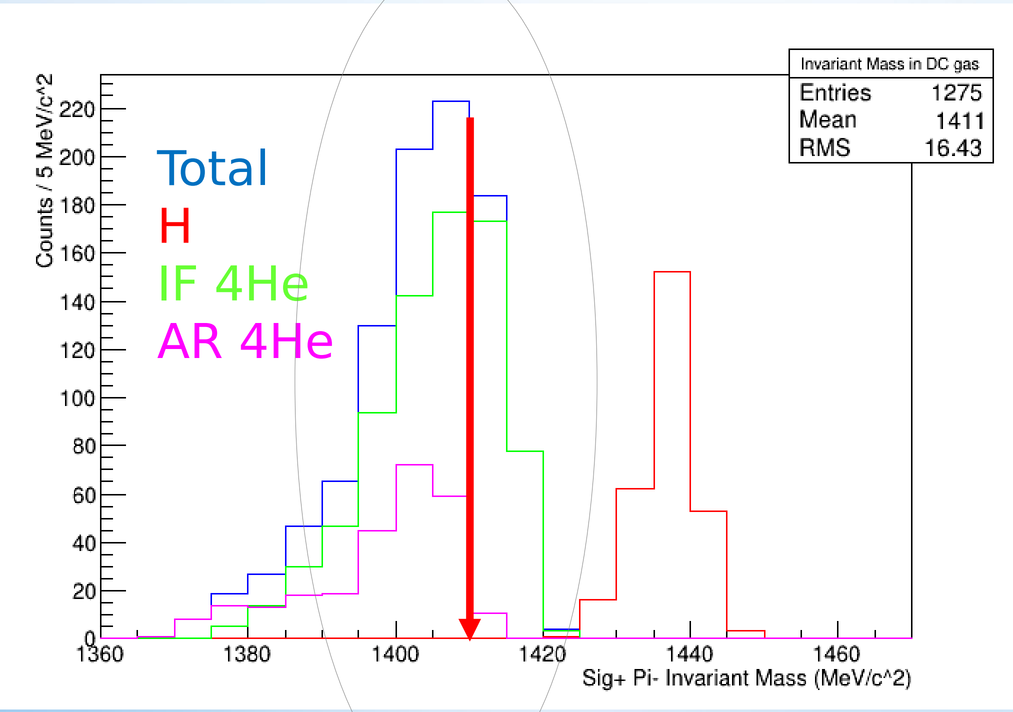


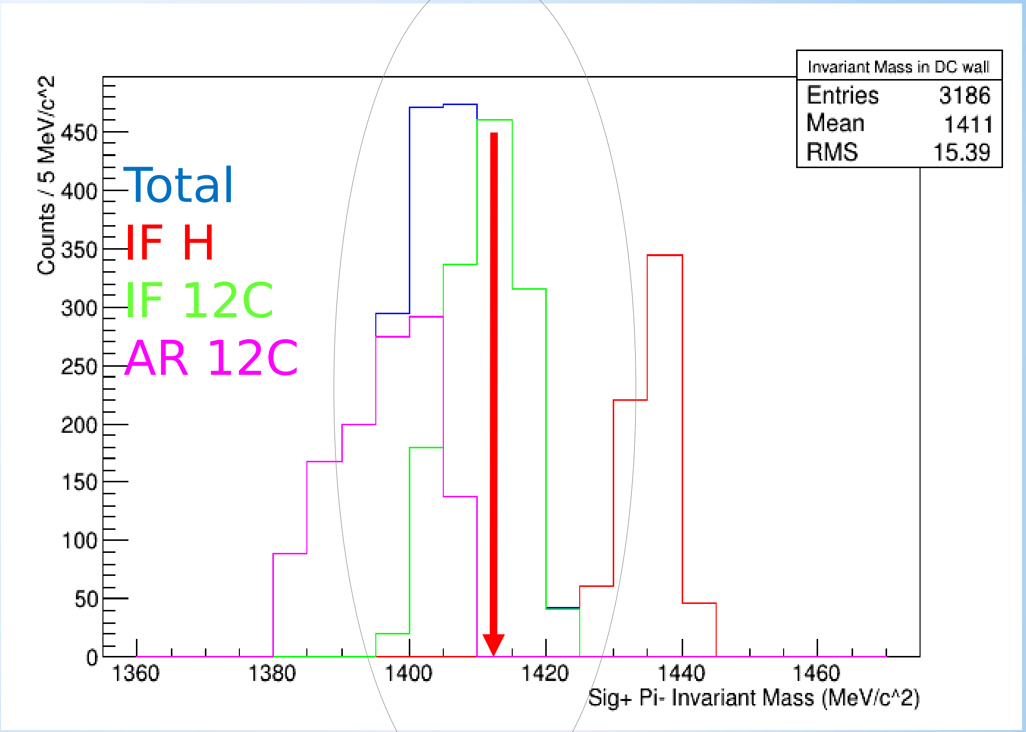

# Resonant VS non-resonant

**$K^- N \rightarrow (Y^* ?) \rightarrow Y \pi$**

**in medium,** how much comes from resonance ?

Non resonant transition amplitude:

- Never measured before below threshold

**(33 MeV below threshold kinetic energy in the Kn CM system):**

$$E_{Kn} = -|B_n| - \frac{p_3^2}{2\mu_{\pi,\Lambda,3He}},$$

- few, old theoretical calculations

(Nucl. Phys. B179 (1981) 33-48)

# Resonant VS non-resonant

Investigated using:

$K^-$"n" $\rightarrow$ $\Lambda\pi^-$ direct formation in $^4He$

the goal is to measure $|f^{N\text{-}R}_{\Lambda\pi}(I=1)|$

to get information on $|f^{N\text{-}R}_{\Sigma\pi}(I=0)|$

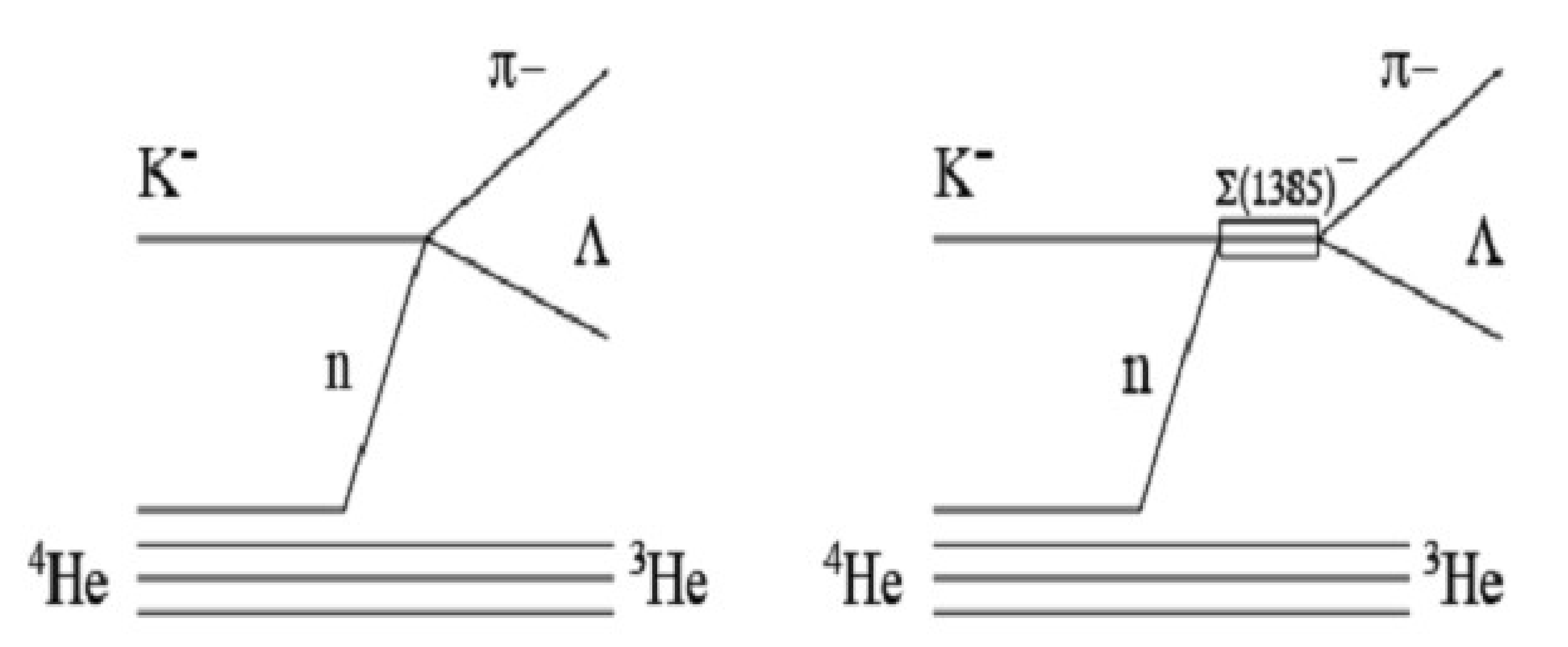

# $K^{-}\ {}^{4}He \rightarrow \Lambda p^{-}\ {}^{3}He$ resonant and non-resonant processes

**Nucl. Phys. A954 (2016) 75-93**

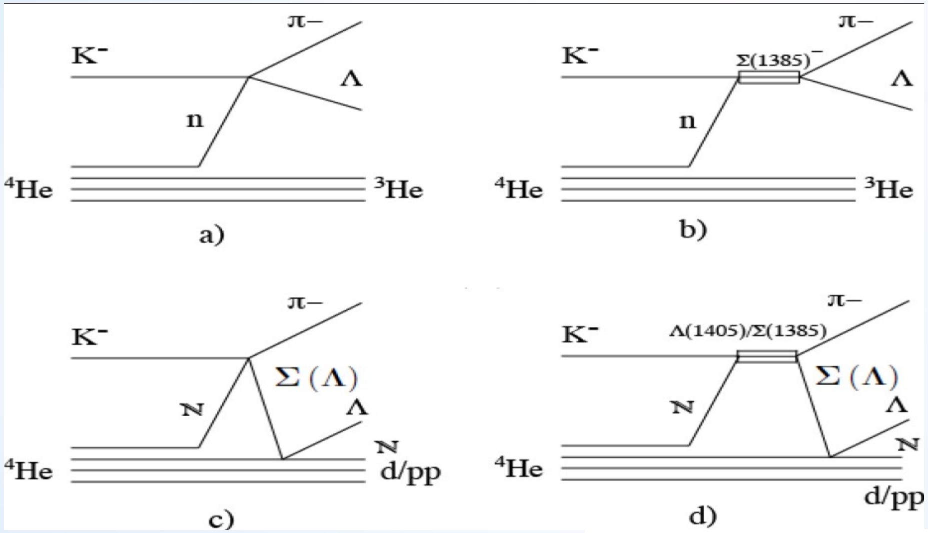


## Theoretical shapes for :

**total $\Lambda\pi^{-}$ momentum spectra for the resonant ($\Sigma^{*-}$) and non-resonant (I = 1) processes were calculated, for both S-state and P-state $K^{-}$ capture at-rest and in-flight. Corrections to the amplitudes due to $\Lambda/\pi$ final state interactions were estimated.**

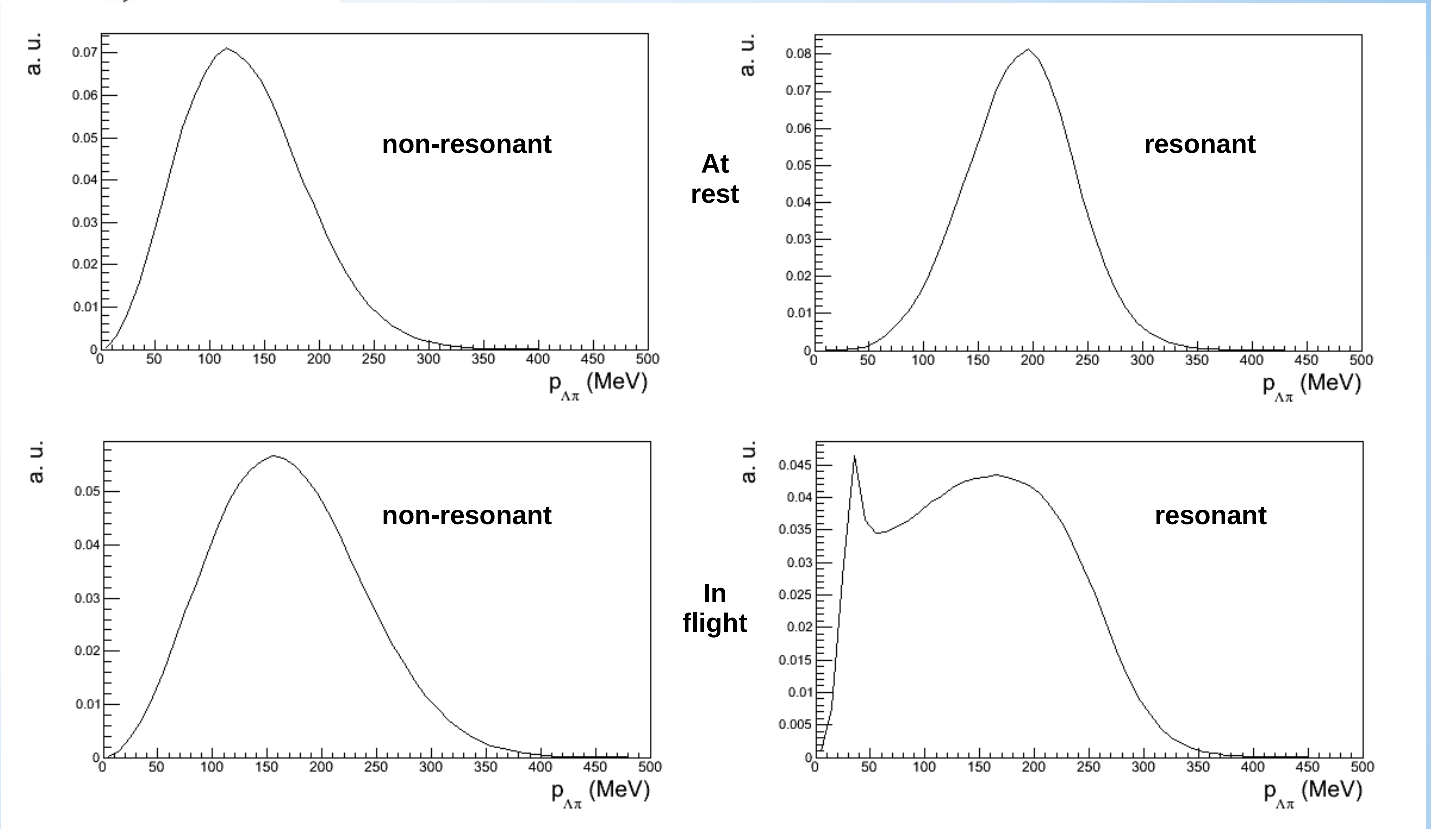


**Collaboration with S. Wycech**

# How to extract the $K^- n \to \Lambda\pi^-$ non resonant transition amplitude

**simultaneous fit ($p_{\Lambda\pi^-}$ - $m_{\Lambda\pi^-}$ - $\cos(\theta_{\Lambda\pi^-})$) with signal and background processes :**

- non resonant $K^-$ capture at-rest from $S$ states in $^4$He
- resonant $K^-$ capture at-rest from $S$ states in $^4$He
- non resonant $K^-$ capture in-flight in $^4$He
- resonant $K^-$ capture in-flight in $^4$He

- primary $\Sigma\pi^-$ production followed by the $\Sigma N \to \Lambda N'$ conversion process
- $K^-$ capture processes in $^{12}$C giving rise to $\Lambda\pi^-$ in the final state

**In order to extract:**

**NR-ar/RES-ar & NR-if/RES-if**

# Results for the $K^- n \to \Lambda\pi^-$ non resonant transition amplitude

| | percentage $\cdot 10^{-2}$ | $\sigma_{stat} \cdot 10^{-2}$ | $\sigma_{syst} \cdot 10^{-2}$ |
|---|---|---|---|
| NR-ar | 12.00 | $\pm$ 1.66 | +1.96 -2.77 |
| RES-ar/NR-ar | 0.39 | $\pm$ 0.04 | +0.18 -0.07 |
| NR-if | 19.24 | $\pm$ 4,38 | +5.90 -3.33 |
| RES-if//NR-if | 0.23 | $\pm$ 0.03 | +0.23 -0.22 |
| $\Sigma \to \Lambda$ conv. | 2.16 | $\pm$ 0.30 | +1.62 -0.83 |
| $K^{-12}$C capture | 57.00 | $\pm$ 1.23 | +2.21 -3.19 |

Table 1. Percentages of the different physical contributions to the selected $\Lambda\pi^-$ sample, from top: non-resonant at-rest, resonant at-rest, non-resonant in-flight, resonant in-flight, $\Sigma N \to \Lambda N'$ conversion processes, $K^-$ absorptions in Carbon. The statistical and systematic errors are shown as well.

**Preliminary**

**extracted:**

**NR-ar/RES-ar & NR-if/RES-if**

# Simultaneous momentum – angle – mass fit

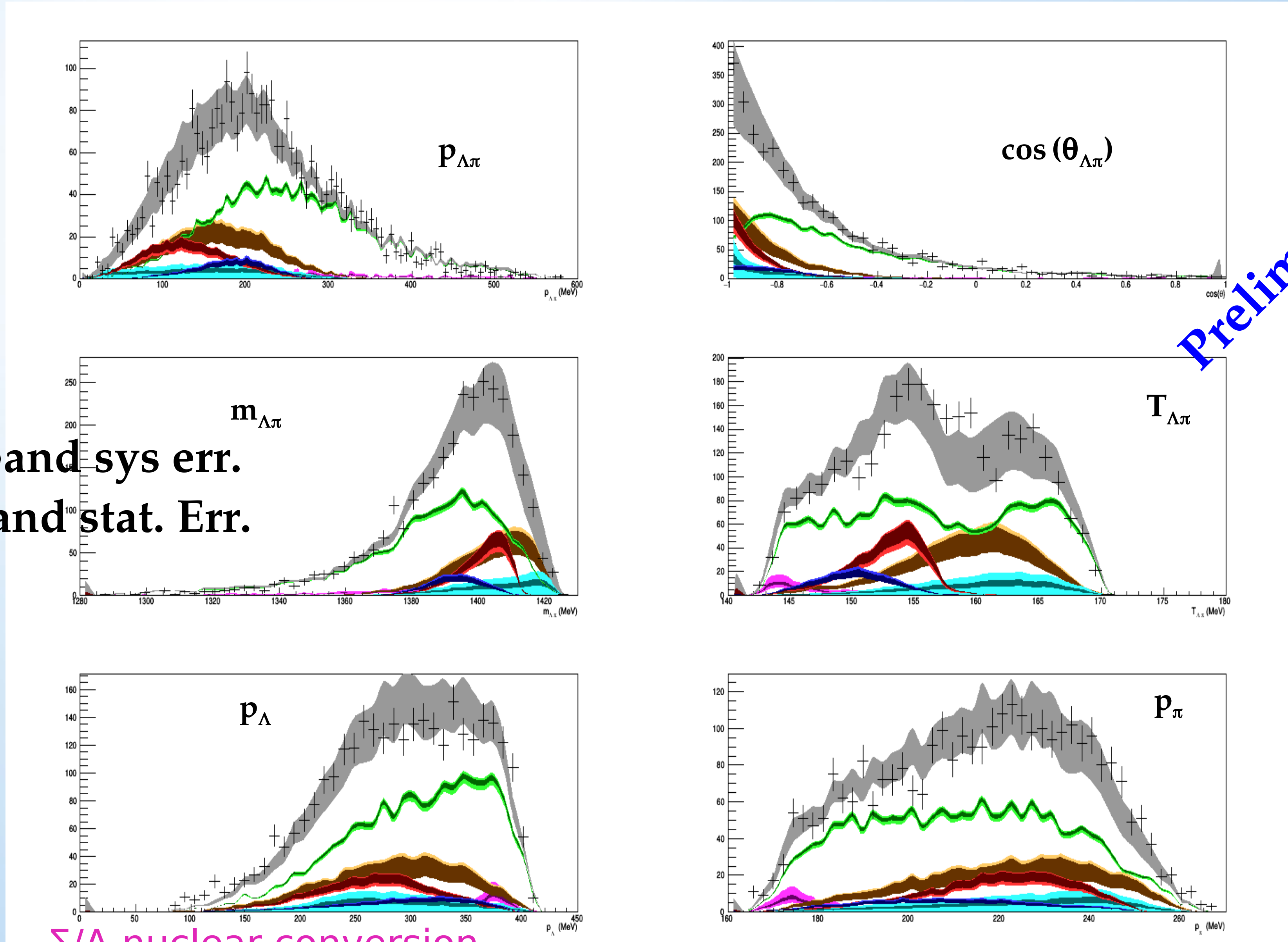


Preliminary

**Light band sys err.**

**Dark band stat. Err.**

Σ/Λ nuclear conversion

K-N→Σ **π**

└→ΣN→**Λ**N'

**Absorptions in 12C (from Carbon wall data)**

# Simultaneous momentum – angle – mass fit

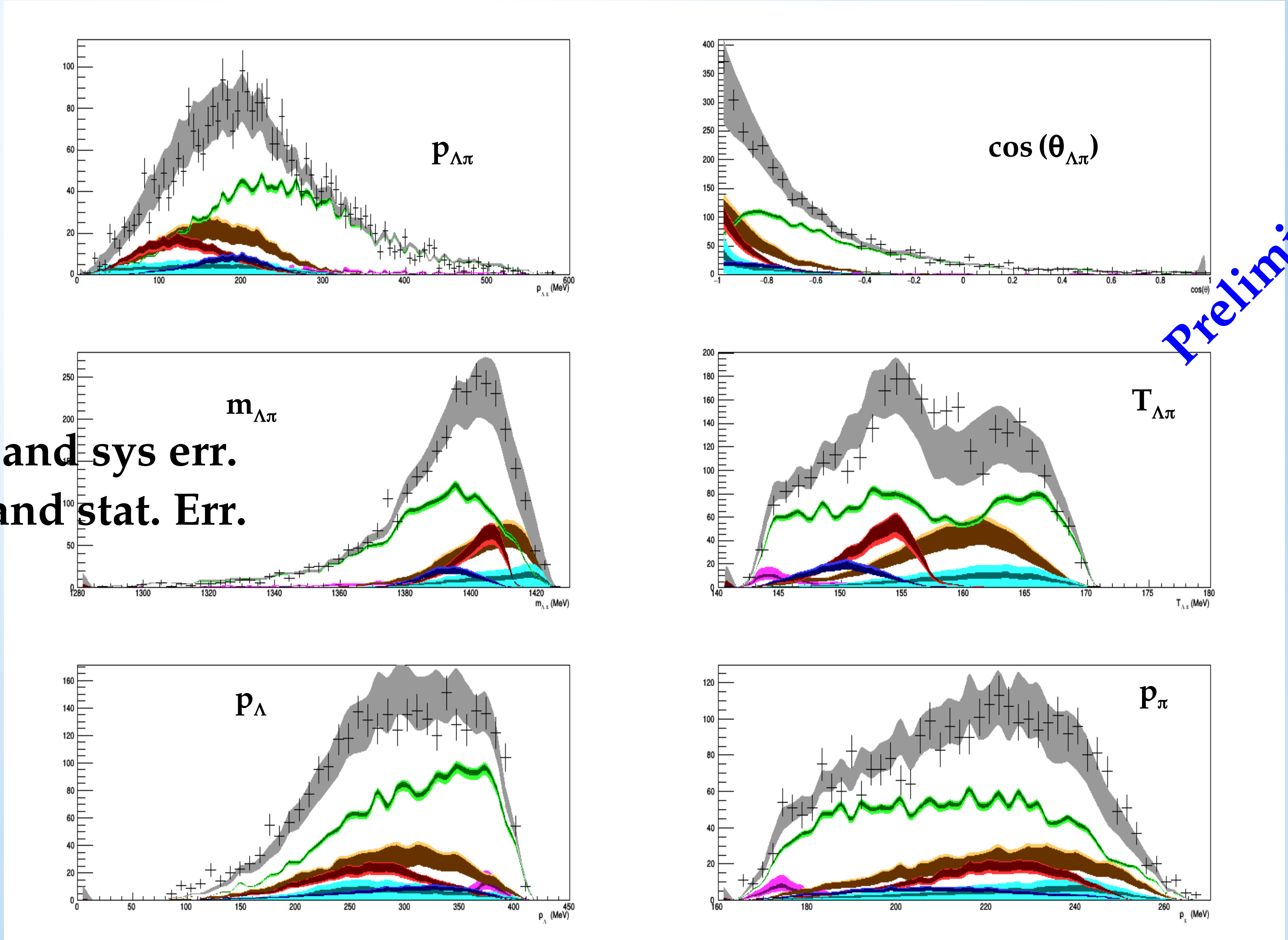


Preliminary

**Light band sys err.**
**Dark band stat. Err.**

**Non-Resonant**
**(at-rest)**
**(in-flight)**

**Resonant $\Sigma*$**
**(at-rest)**
**(in-flight)**

# Comparison

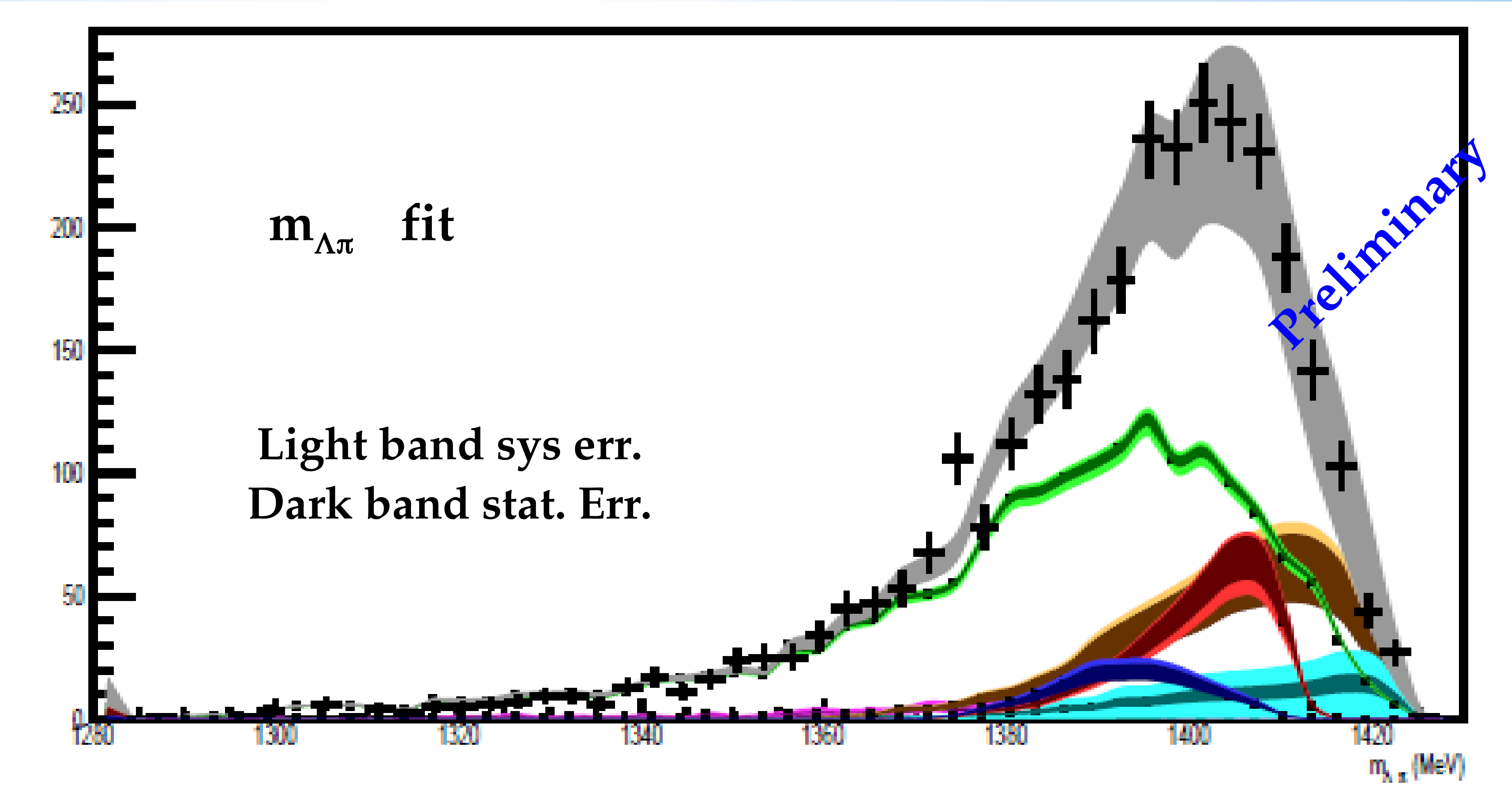


**Non-Resonant**
**(at-rest)**
**(in-flight)**

**Resonant Σ***
**(at-rest)**
**(in-flight)**

# Outcome of the measurement

**From the well known Σ* transition probability:**

*Preliminary*

$$\frac{\int_0^{pmax} P_s^s(p_{\Lambda\pi})\, dp_{\Lambda\pi}}{\int_0^{pmax} P_s^p(p_{\Lambda\pi})\, dp_{\Lambda\pi}} = |f_{ar}^s|^2 \cdot 8,94 \cdot 10^5 MeV^2.$$

Using the measured value for the ratio $\frac{NR-ar}{RES-ar}$, the module of the non resonant transition amplitude is found to be:

$$|f_{ar}^s| = (0.334 \pm 0.018 stat^{+0.34}_{-0.58} syst)\ \text{fm}. \qquad (27)$$

**The sub-threshold result is compatible with corresponding values extracted from $K^-$ p → Λ $\pi^0$ cross sections above threshold**

**J. K. Kim, Columbia University Report, Nevis 149 (1966)**

**J. K. Kim, Phys Rev Lett, 19 (1977) 1074:**

| $E = -33 MeV$ | $p_{lab} = 120\ MeV$ | 160 MeV | 200 MeV | 245 MeV |
|---|---|---|---|---|
| $0.334 \pm 0.018 stat^{+0.034}_{-0.058} syst$ | 0.33(11) | 0.29(10) | 0.24 (6) | 0.28(2) |

$K^-$

# future AMADEUS physics case

# $K^-$ N cross section measurement below $p_K$=100 MeV/c , example..

- $K^-$ p → $\Sigma^0\pi^0$ cross section measurement at or below 100 MeV/c missing

- existing data at (120, 160, ..) MeV/c with big relative errors (about 50% & 120 MeV/c)

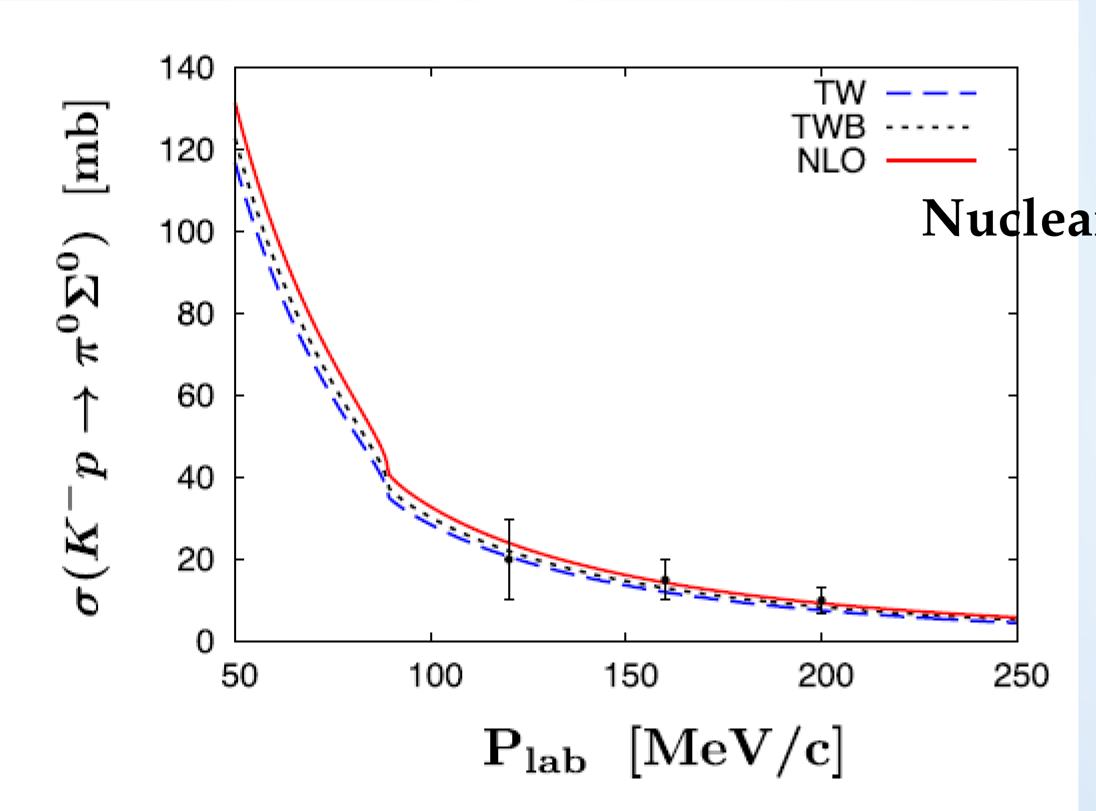


Nuclear Physics A 881 (2012) 98–114

# $K^- p \rightarrow \Sigma^0\pi^0$ cross section measurement can be done

- K- H capture at-rest → kinematics is closed
- K- H capture at-rest ($p_K$ = 90 MeV) → kinematics is closed
- K- H capture at-rest ($p_K$ = 100 MeV) → kinematics is closed
- K- 4He capture at-rest + in-flight ($l_K$ = 1)
- K- 12C capture at-rest + in-flight ($l_K$ = 2, valence proton)

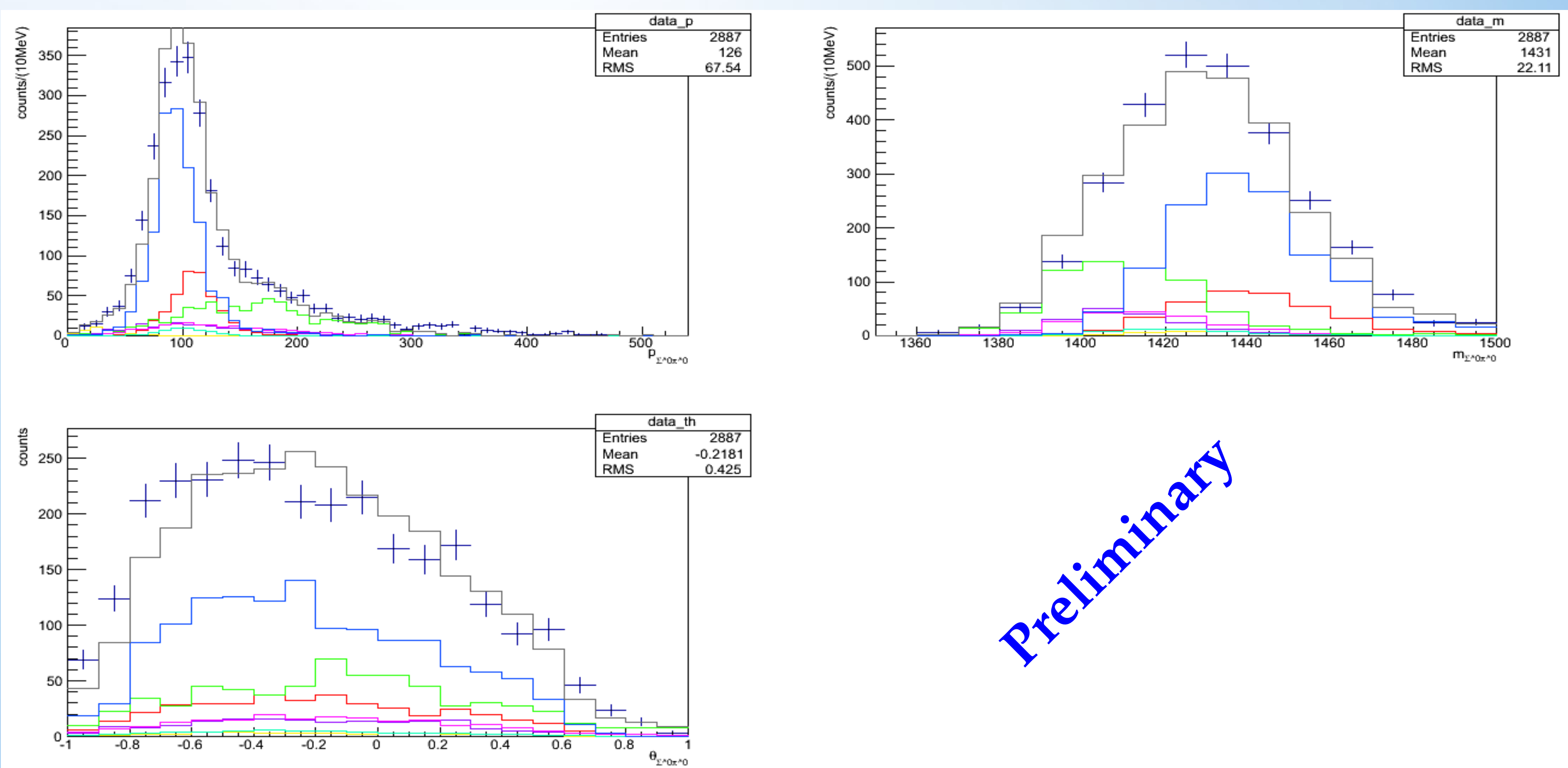

# Λ(1405) from K- induced reactions on deuterons

- Extract the Λ(1405) resonance shape from **K- induced reactions on deuterons** (resonance is produced by the KN channel) **in-fight** (with $p_K$ = 130 MeV/c)

- Calculations performed for these particular reactions based on the Esmaili - Akaishi - Yamazaki framework [Phys. Rev. C 83, (2011)] (left)

greatly differ from chiral predictions [Eur. Phys. J. A 42, 257 (2009)] & [Eur. Phys. J. A (2011) 47] (right)

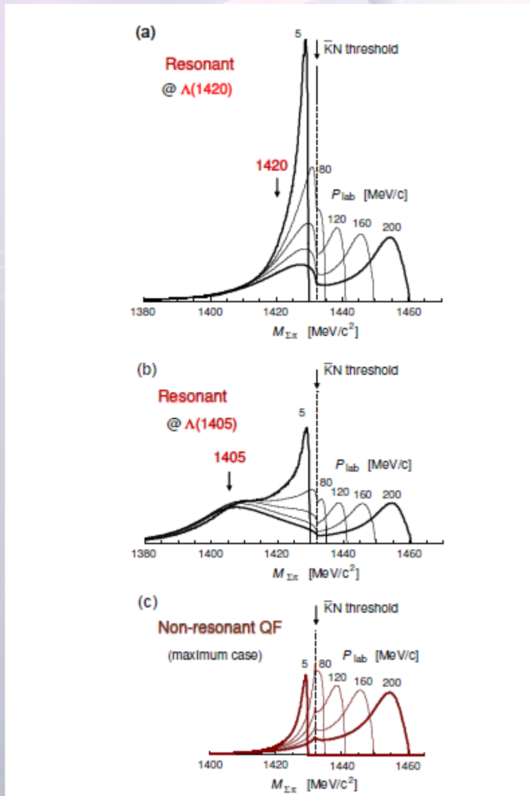


Figure 6: $T_{21}$ $\Sigma\pi$ invariant-mass spectra from low-momentum $K^- + d$ reactions calculated with AY interactions. The total spectra (resonant plus non-resonant): (a) for AY 1432-34 and (b) for AY 1405-30. The curves (a) and (b) are normalized to unit area to compare with $K^- d$ atomic absorption. (c) The case of non-resonant QF contribution for (a), in which the resonant QF contributions via $\Lambda^*$ are subtracted by reducing $U_{11}$ to $0.59\,U_{11}$ where the $\Lambda^*$ quasi-bound state disappears.

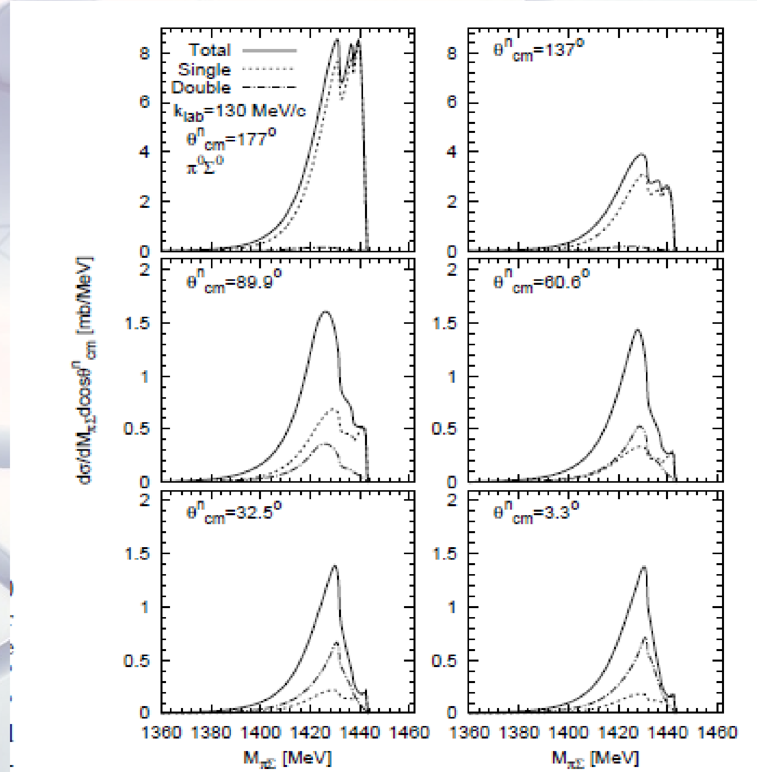


**Fig. 5.** Differential $\pi\Sigma$ invariant mass spectra of $K^- d \to \pi^0 \Sigma^0 n$ for 130 MeV/c of incident $K^-$ momentum fixing the angle between the emitted neutron and the incident $K^-$ in the CM frame. In each panel, the solid line denotes the total contributions of the three diagrams, while the dotted and dash-dotted lines show the calculations from the single and double scatterings, respectively.

# detection of neutrals:

$K^-$

- Extract the $\Sigma^0\pi^0$ spectra:

  free from $\Sigma(1385)$ background I=1

- The kinematics of the K- d $\rightarrow \Sigma^0\pi^0$ n reaction would be closed with the neutron detection $\rightarrow$ **event by event separation of at-rest from in-fight K- nuclear captures.**

- The selection of forward neutrons (angle between the outgoing neutron and the incident K- in the CM frame) drastically reduces the contribution of the single scattering, resonant (1405) formation dominates.

# Y-N/NN interaction essential impact on the case of NEUTRON STARS


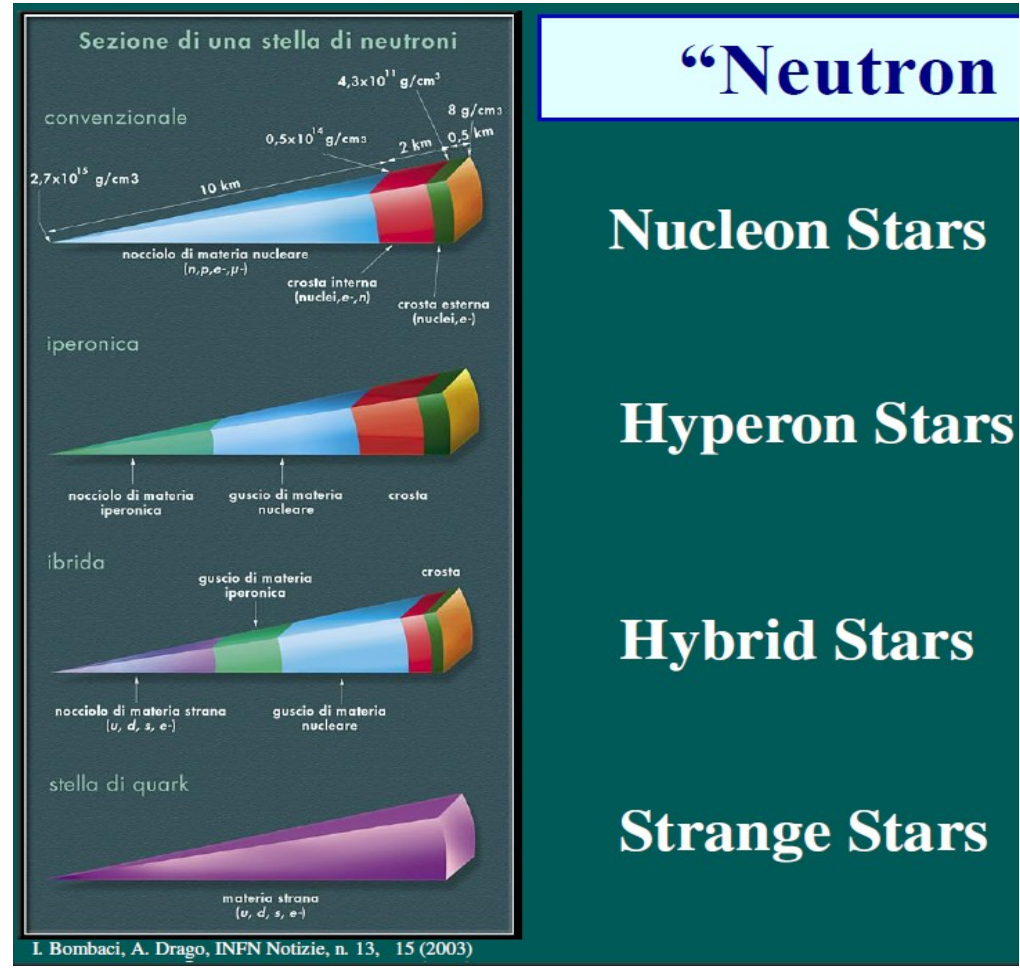


**Microscopic approach to hyperonic matter EOS**

input

**2BF:** nucleon-nucleon (NN), nucleon-hyperon (NY), hyperon-hyperon (YY)
e.g. Nijmegen, Julich models

**3BF:** NNN, NNY, NYY, YYY

**Hyperonic sector: experimental data**

1. YN scattering (very few data)
2. Hypernuclei

# No experimental information on $\Sigma^0$-N/NN interaction

## Λ-neutron matter

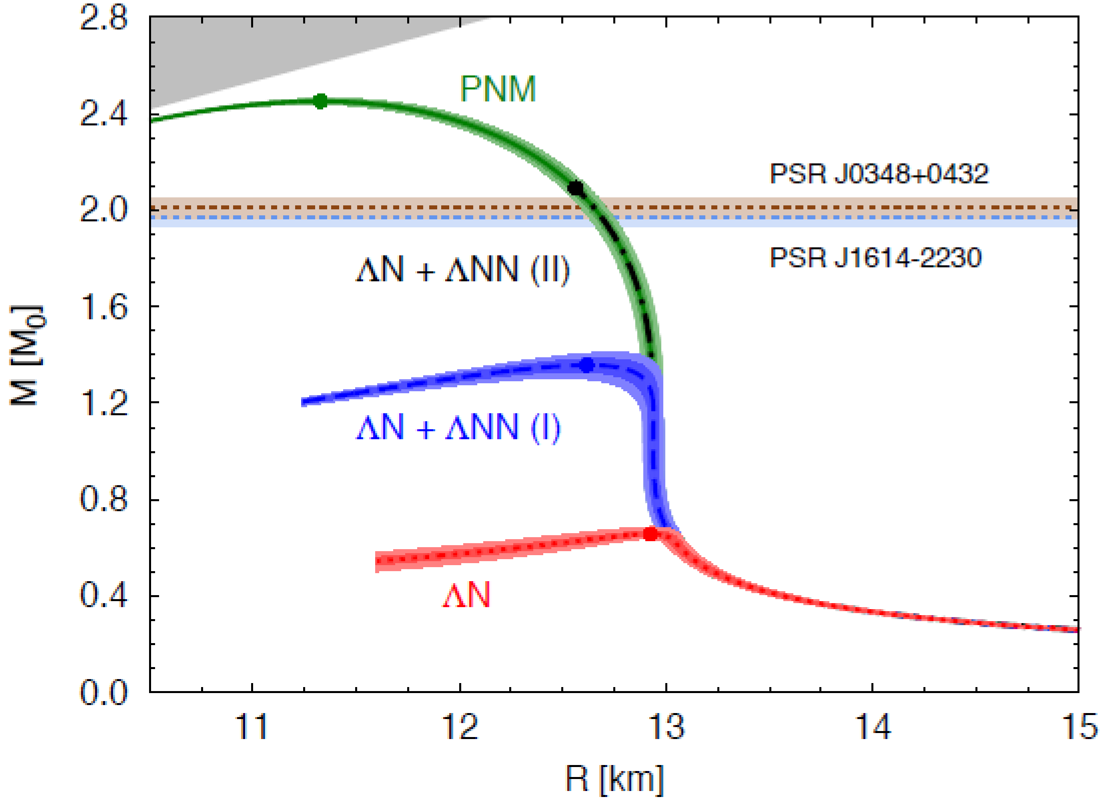


Lonardoni, Lovato, Gandolfi, Pederiva, PRL (2015)

Drastic role played by $\Lambda NN$. Calculations can be compatible with neutron star observations.

Note: no $v_{\Lambda\Lambda}$, no protons, and no other hyperons included yet...

# No experimental information on $\Sigma^0$-N/NN interaction

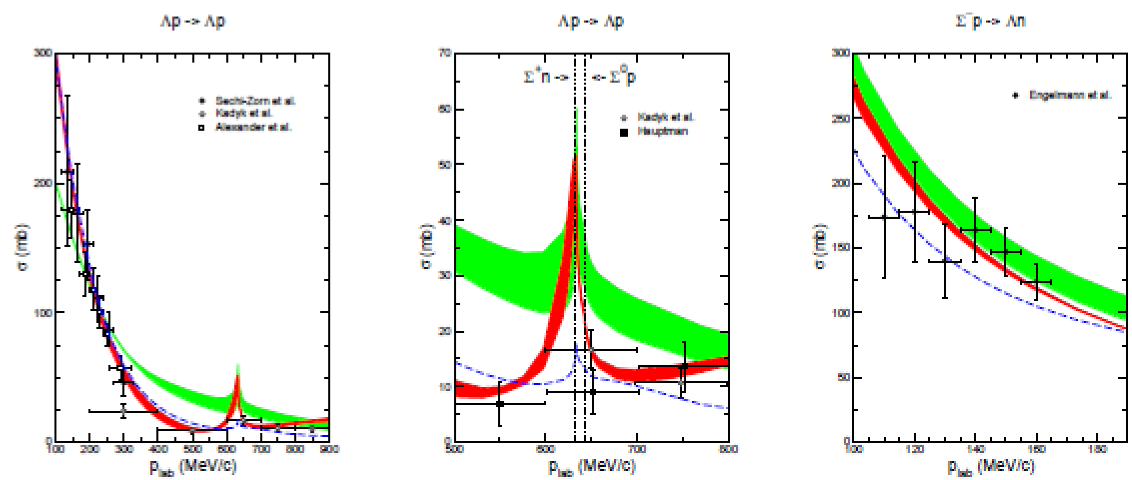


**Nucl. Phys. A 915 (2013) 24-58**

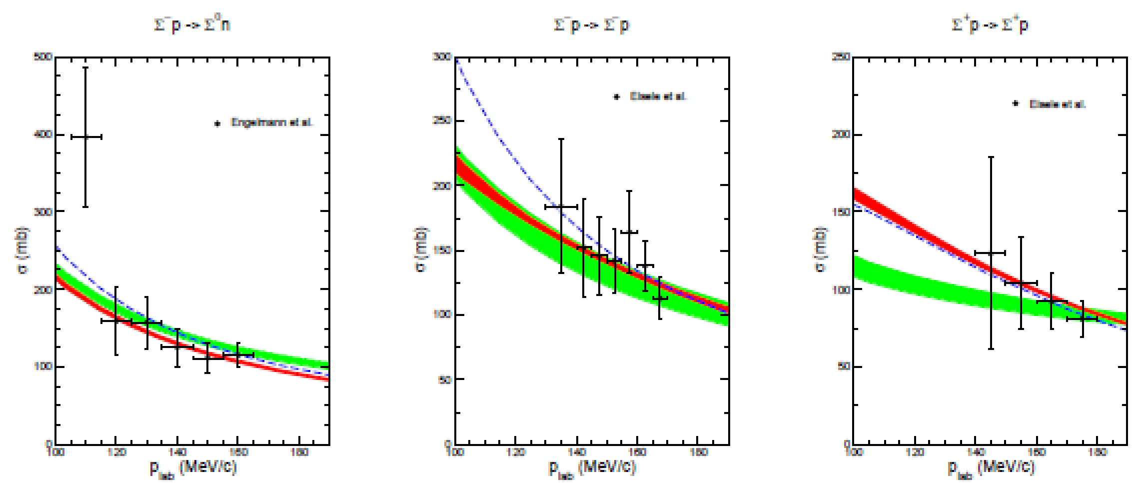


Figure 2: "Total" cross section $\sigma$ (as defined in Eq. (24)) as a function of $p_{\rm lab}$. The experimental cross sections are taken from Refs. [52] (filled circles), [53] (open squares), [65] (open circles), and [66] (filled squares) ($\Lambda p \to \Lambda p$), from [54] ($\Sigma^- p \to \Lambda n$, $\Sigma^- p \to \Sigma^0 n$) and from [55] ($\Sigma^- p \to \Sigma^- p$, $\Sigma^+ p \to \Sigma^+ p$). The red/dark band shows the chiral EFT results to NLO for variations of the cutoff in the range $\Lambda = 500, \ldots, 650$ MeV, while the green/light band are results to LO for $\Lambda = 550, \ldots, 700$ MeV. The dashed curve is the result of the Jülich '04 meson-exchange potential [36].

**$(K^{-}\ ppn) + n \rightarrow \Sigma^0\ d + n$**

**3NA in $^4He$**

**for the investigation of the**

**$\Sigma^0$-N & $\Sigma^0$-(NN) interaction**

# 3NA - $(K^{-}\,ppn) + n \rightarrow \Sigma^{0}\,d + n$

**3NA can be followed by two possible elastic FSI**

1) $n\,d \rightarrow n\,d$ we may take advantage of the well known $\sigma$NN data

2) $\Sigma^{0}\,n/d \rightarrow \Sigma^{0}\,n/d$ from which to estract information on $\Sigma^{0}$-N , $\Sigma^{0}$-(NN) interaction.

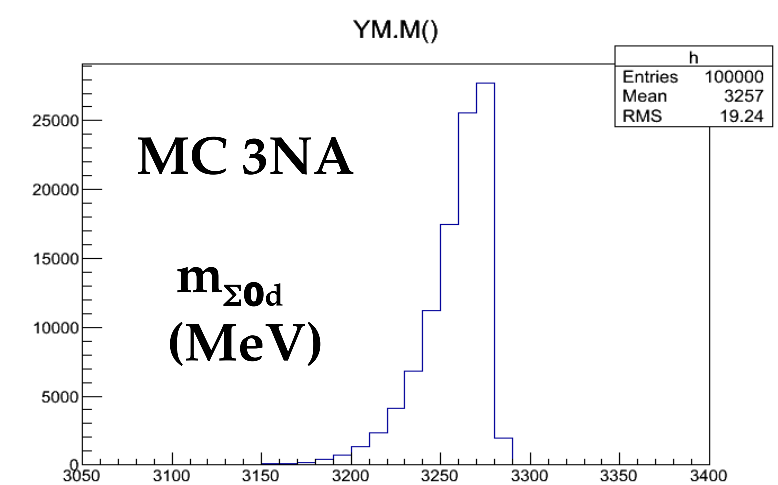


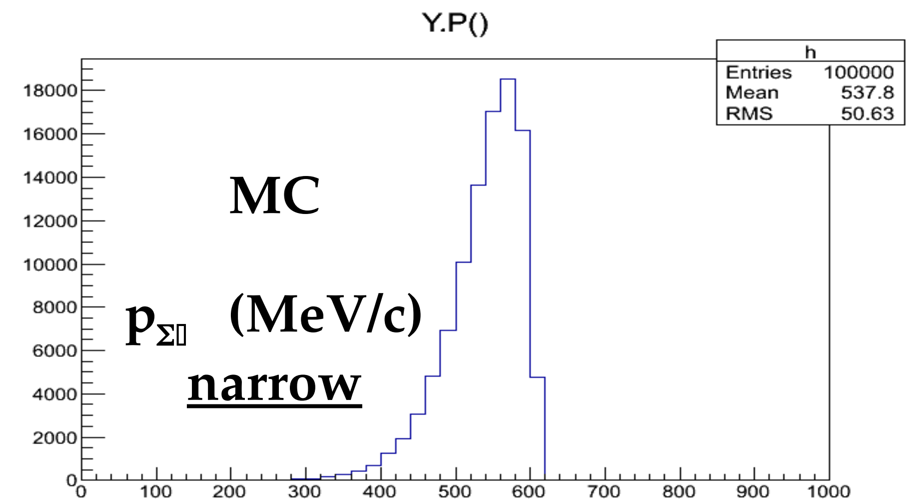


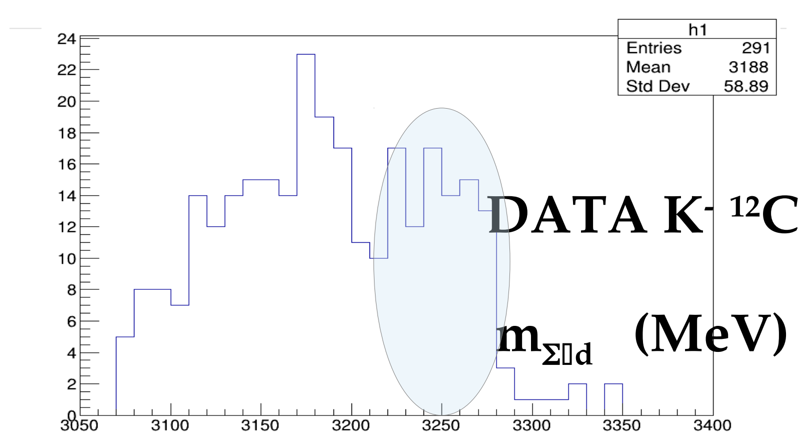


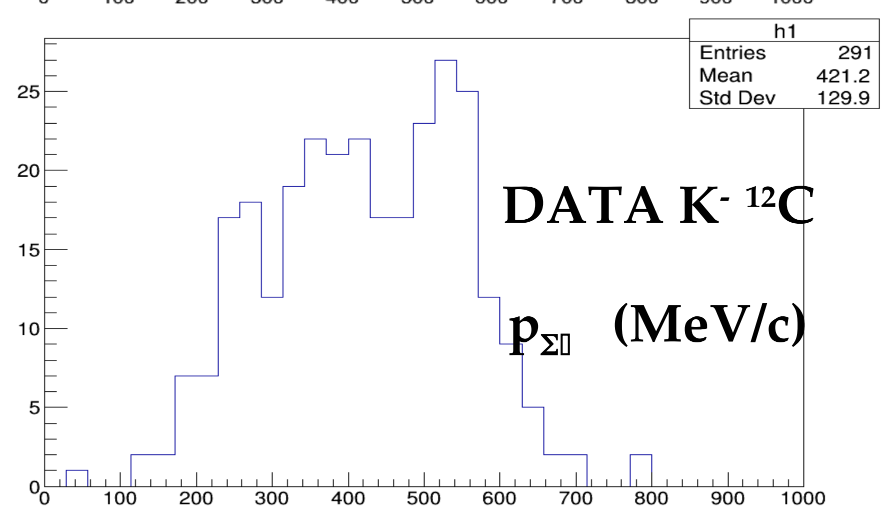

# 2NA - $(K^- pn) + d \rightarrow \Sigma^0 n + d$

## 2 possible elastic FSI

1) $n\, d \rightarrow n\, d$ we may take advantage of the well known $\sigma_{NN}$ data

2) $\Sigma^0\, d/n \rightarrow \Sigma^0\, d/n$ *hopefully well separated in the lower energy part of the final state phase space*

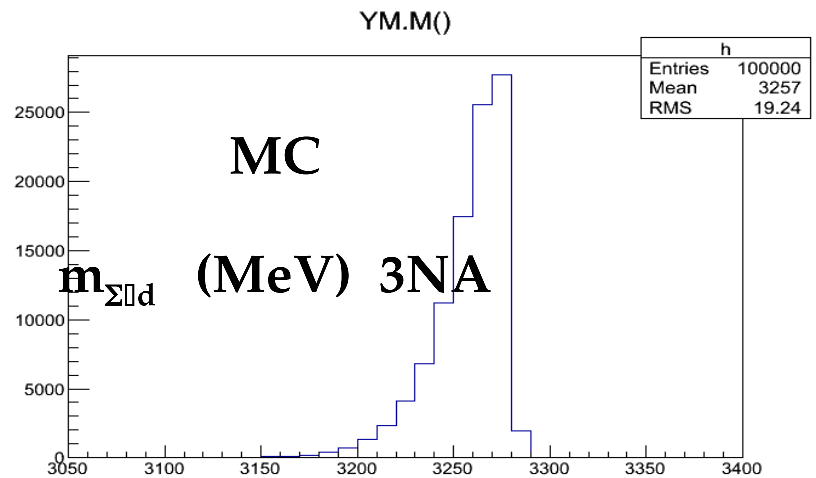


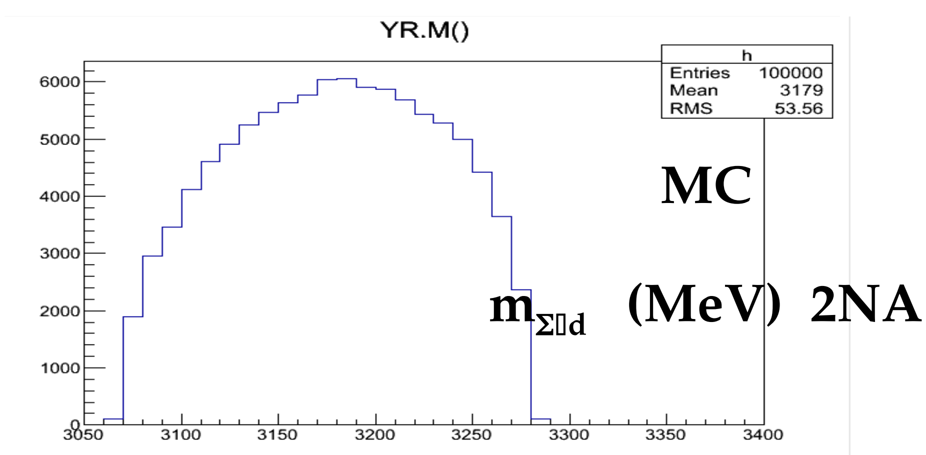

**Accurate model of the:**

$$(K^- \; ppn) + n \rightarrow \Sigma^0 \, d + n$$

**3NA in $^4$He**

**+**

$$\Sigma^0 \, d/n \rightarrow \Sigma^0 \, d/n \quad \text{FSI}$$

**is needed to extract the corresponding cross sections from the measured shapes.**


$K^-$
Thanks